Physics in Medicine & Biology

IPEM
Institute of Physics and
Engineering in Medicine

TOPICAL REVIEW

Source-detector trajectory optimization in cone-beam computed tomography: a comprehensive review on today's state-of-the-art

S Hatamikia[1,2,3] , A Biguri[4] , G Herl[5], G Kronreif[1], T Reynolds[6] , J Kettenbach[7], T Russ[8] , A Tersol[9],
A Maier[10] , M Figl[3], J H Siewerdsen[9] and W Birkfellner[3]

[1] Austrian Center for Medical Innovation and Technology (ACMIT), Wiener Neustadt, Austria
[2] Research center for Medical Image Analysis and Artificial Intelligence (MIAAI), Department of Medicine, Danube Private University, Krems, Austria
[3] Center for Medical Physics and Biomedical Engineering, Medical University of Vienna, Vienna, Austria
[4] Department of Applied Mathematics and Theoretical Physics, University of Cambridge, Cambridge, United Kingdom
[5] Deggendorf Institute of Technology, D-94469 Deggendorf, Germany
[6] University of Sydney, Australia
[7] Institute of Diagnostic, Interventional Radiology and Nuclear Medicine, Landesklinikum Wiener Neustadt, Wiener Neustadt, Austria
[8] Computer Assisted Clinical Medicine, Heidelberg University, Heidelberg, Germany
[9] Department of Biomedical Engineering, Johns Hopkins University, United States of America
[10] Pattern Recognition Lab, University of Erlangen-Nuremberg, D-91054 Erlangen, Germany

E-mail: sepideh.hatamikia@acmit.at

Abstract

Cone-beam computed tomography (CBCT) imaging is becoming increasingly important for a wide range of applications such as image-guided surgery, image-guided radiation therapy as well as diagnostic imaging such as breast and orthopaedic imaging. The potential benefits of non-circular source-detector trajectories was recognized in early work to improve the completeness of CBCT sampling and extend the field of view (FOV). Another important feature of interventional imaging is that prior knowledge of patient anatomy such as a preoperative CBCT or prior CT is commonly available. This provides the opportunity to integrate such prior information into the image acquisition process by customized CBCT source-detector trajectories. Such customized trajectories can be designed in order to optimize task-specific imaging performance, providing intervention or patient-specific imaging settings. The recently developed robotic CBCT C-arms as well as novel multi-source CBCT imaging systems with additional degrees of freedom provide the possibility to largely expand the scanning geometries beyond the conventional circular source-detector trajectory. This recent development has inspired the research community to innovate enhanced image quality by modifying image geometry, as opposed to hardware or algorithms. The recently proposed techniques in this field facilitate image quality improvement, FOV extension, radiation dose reduction, metal artifact reduction as well as 3D imaging under kinematic constraints. Because of the great practical value and the increasing importance of CBCT imaging in image-guided therapy for clinical and preclinical applications as well as in industry, this paper focuses on the review and discussion of the available literature in the CBCT trajectory optimization field. To the best of our knowledge, this paper is the first study that provides an exhaustive literature review regarding customized CBCT algorithms and tries to update the community with the clarification of in-depth information on the current progress and future trends.

1. Introduction

Ever since the introduction of modern tomographic imaging techniques in nuclear medicine (Kuhl and Edwards 1970, Muehllehner 1971, Muehllehner and Wetzel 1971, Jaszczak 2006) and, above all, x-ray imaging (Hounsfield 1973, Peters *et al* 1973, Maier *et al* 2018, Noo and Kachelriess 2019), reconstruction was at the center

of this research. Soon after the laconic presentation of solving the inverse problem as linear equations in Hounsfield (1973), the importance of more advanced functional approaches developed earlier Radon (1917), Cormack (1963) became evident, and a plethora of related research works on reconstruction techniques was published ever since then Fessler (2013).

To reconstruct a two-dimensional slice, it makes sense in computed tomography (CT) to choose the trajectory of an x-ray source and the detector array in such a way that both orbit a common isocenter. This trajectory is not ideal for the analysis of three-dimensional structures, as it does not generate sufficient information for three-dimensional reconstruction Tuy (1983). However, since it is comparatively straightforward to apply, the overwhelming majority of transmission tomographic systems follow this geometry. This holds true for all major developments in CT, starting in the early days fifty years ago over the introduction of more powerful or efficient imaging geometries. In addition motion patterns such as spiral CT Kalender *et al* (1990), multislice CT (which was already envisioned in Hounsfield (1973) but realized by Elscint not earlier than 1992 Seifert *et al* 1997) and cone-beam CT (CBCT) (Pelc and Chesler 1979, Feldkamp *et al* 1984) followed such conventional geometry. Numerous accounts on the development of tomographic imaging and various types of reconstruction techniques emerged in the past decades (Gordon and Herman 1974, Webb 1990, Kak and Slaney 2001, Buzug 2010).

The use of free-form imaging geometries, on the other hand, has only received little attention. Yet there are developments aiming at freehand single photon emission computed tomography (SPECT) systems which provide additional diagnostic quality in an interventional suite (Kleinjan *et al* 2016); an unconstrained cone-beam computed tomography (CBCT) system, however, could also add substantial clinical benefit. Interventional imaging provides an ideal experimental field to customize source-detector trajectories to the patient and to optimize diagnostic task for several reasons: a prior interventional image (CT or CBCT) for most of patients usually exists,these provide a detailed representation of the patient anatomy. Furthermore, the imaging target including the specific region of interest and particular image features to be reconstructed or localized tend to be very well defined and finally, additional information, including the location and sizes of implants or tools and the treatment planning is known prior to the intervention.

The advent of x-ray based robotic interventional systems has opened the door to significantly increased flexibility in the design of CBCT acquisition orbits. A breadth of alternative CBCT trajectories—which can all be theoretically implemented on such a robotic C-arm CBCT as well as novel multi-source CBCT systems- has thus been investigated recently in order to address various issues in the clinical scenarios: non-circular, tilted, multi-circle and sinusoidal orbits of various frequencies and combinations of them to improve image quality (Stayman and Siewerdsen 2013, Gang *et al* 2015, Boone *et al* 2019, Stayman *et al* 2019, Gang *et al* 2020, Thies *et al* 2020, Wu *et al* 2020), a combination of multiple arcs to avoid interfering structures (Meng *et al* 2013, Hatamikia *et al* 2020, 2020, Hatamikia 2021), circular tomosynthesis to reduce the imaging dose (Chung *et al* 2018) and reverse helical orbits, line-ellipse-line and multiple parallel circular orbits to increase the field-of-view as well as reduction in cone-beam artifacts (Yu *et al* 2013, 2014, 2015, 2016, Gang *et al* 2018, Boone *et al* 2019, Reynold *et al* 2021). One may also imagine very compact x-ray tube/detector combinations which cover a volume by means of combined motions in both 3D rotation and translation, or the combination of sources and detectors mounted to independent robotic devices.

This review focuses on the published strategies to optimize CBCT trajectories in non-conventional computed tomography; both trajectory optimization techniques and the special goal they were designed for are presented.

2. Developments on trajectory optimization in CBCT

The additional flexibility provided by robotic CBCT systems allows for implementation of more general source-detector trajectories which are beyond the traditional circular and helical trajectories that have been the standard for CBCT imaging since decades. The non-conventional trajectories were initially mainly employed to address the field of view (FOV) and the sampling issues in interventional CBCT. For instance, non-circular trajectories were used to improve 3D sampling and to permit extended axial and elliptical FOVs in order to reduce the artifacts arising from standard circular CBCT trajectory. Tilted circular orbits were also used due to their superior performance in improving the image quality and target localization for instance to improve the image quality adjacent to the skull base and to improve localization in CT-guided biopsies. During the last decade, several studies have suggested modifications of the orbit beyond simple tilts by means of optimizing non-conventional CBCT trajectories and have reported several clinical advantages using this approach. In this section we propose different categorization of the available literature on non-conventional CBCT trajectory design according to their final goal in performing the trajectory optimization. In addition, we provide table 1 which

Table 1. Categorization of different studies according to different factors including main application, goal of the study, prior knowledge, trajectory parameterization, objective function and the optimization approach.

	Categorization					
Study	Main application	Goal	Prior knowledge	Trajectory parameterization	Objective function	Optimization approach
Stayman (Stayman and Siewerdsen 2013)	Interventional imaging	Task-based image quality improvement	Prior CT	Arbitrary sets of views on a spherical orbit	NPWMF detectability index	Greedy optimization
Gang (Gang et al 2015)	Interventional imaging	Task-based image quality improvement	Prior CT	Tilted orbits	NPWMF detectability index	Gradient-based optimization
Stayman (Stayman et al 2015)	Interventional imaging	Task-based image quality improvement	Prior CT	Tilt angle for every rotation angle	NPWMF detectability index	CMA-ES
Stayman (Stayman et al 2019)	Interventional imaging	Task-based image quality improvement	Prior CT	Compositions of basis functions by using B-Splines	NPWMF detectability index	CMA-ES
Hatamikia (Hatamikia et al 2020)	Interventional imaging	collision avoidance and dose reduction	Prior CT	Combinations of two short arcs	FSIM	Brute force
Amirkhanov (Amirkhanov et al 2010)	Object position optimisation in industry	Image quality improvement at the surface, dimensional metrology	CAD file of the object	Tilted orbits	Radon analysis of the surface, penetration lengths of x-rays	Brute force
Schielein (Schielein et al 2016)	Object position optimization in industry	Overall image quality improvement	CAD file of the object	Tilted orbits	Shannon entropy from the reconstructed image	Brute force
Grozmani (Grozmani et al 2019)	Object position optimization in industry	Overall and local image quality improvement	CAD file of the object	Tilted orbits	Estimation of the CNR from simulated projections	Brute force
Brierely (Brierley et al 2018)	Multi-shot imaging for defect detection	Optimal defect detection	CAD file of the object, expected defects	Arbitrary views	CNR of expected defects	Genetic Algorithm
Fischer (Fischer et al 2016)	Twin-robotic CBCT in industry	Task-based image quality improvement	CAD file of the object	Arbitrary views	NPWMF observer	Greedy
Bauer (Bauer et al 2020)	Twin-robotic CBCT in industry	Reduction of scan time	CAD file of the object	Arbitrary views	Sparsity of Fourier coefficients of the reconstructed volume	Brute force
Herl (Herl et al 2020)	Twin-robotic CBCT in industry	Local image quality improvement	CAD file of the object	Arbitrary views	Data completeness	Greedy
Herl (Herl et al 2021)	Twin-robotic CBCT in industry	Local, task-based image quality improvement	CAD file of the object	Arbitrary views	Data completenss, NPWMF observer	Greedy
Wu (Wu et al 2020)	Image-guided surgery	Metal artifact reduction	No exact prior information required	Tilted circular and non-circular orbits	Map of spectral shift	CMA-ES
Hatamikia (Hatamikia et al 2021)	Interventional imaging	Collision avoidance	Prior CT	Combinations of three short arcs	FSIM	Brute force and heuristic
Gang (Gang et al 2020)	Interventional imaging	Metal artifact reduction	No prior knowledge	Tilted circular and a sinusoidal orbit	Local completeness metric	CMA-ES
Thies (Thies et al 2020)	Interventional imaging	Metal artifact reduction	Neighboring projections	Non-circular orbit	Detectability index	Brute force

Table 2. Summary of the proposed methods for CBCT FOV extension.

Study	Year	Goal	Approach
Zeng (Zeng and Gullberg 1992)	1992	Longitudinal FOV extension	Circle-and-line orbit
Kohler (Kohler *et al* 2001)	2001	Longitudinal FOV extension	Parallel circular trajectories
Manhart (Manhart *et al* 2010)	2010	Lateral FOV extension	Offset detector
Li (Li *et al* 2010)	2010	Lateral FOV extension	Elliptical trajectory
Yu (Yu *et al* 2011)	2011	Longitudinal FOV extension	Line plus arc trajectory
Yu (Yu *et al* 2011)	2011	Longitudinal FOV extension	Reverse helical trajectory
Tan (Tan *et al* 2012)	2012	Longitudinal FOV extension	Helical trajectory
Zheng (Zheng *et al* 2012)	2012	Longitudinal FOV extension	Double orbit
Yu (Yu *et al* 2014)	2014	Longitudinal FOV extension	Reverse helical trajectory
Yu (Yu *et al* 2014)	2014	Longitudinal FOV extension	Multi-turn reverse helix trajectory
Yang (Yang *et al* 2014)	2014	Lateral FOV extension	Complementary circular scan
Herbst (Herbst *et al* 2015)	2015	Lateral FOV extension	Dynamic detector offset
Yu (Yu *et al* 2015)	2015	Longitudinal FOV extension	Reverse helix trajectory
Stromer (Stromer *et al* 2016)	2016	Lateral FOV extension	Rotated detector
Yu (Yu *et al* 2016)	2016	Longitudinal FOV extension	Line-ellipse-line trajectory
Gang (Gang *et al* 2018)	2018	Longitudinal FOV extension	Multi x-ray source
Boone (Boone *et al* 2019)	2019	Longitudinal FOV extension	Multi x-ray source
Rafic (Mohamathu Rafic *et al* 2019)	2019	Longitudinal FOV extension	Two circles with table translation
Guo (Guo *et al* 2020)	2020	Longitudinal FOV extension	Extended line-ellipse-line trajectory
Becker (Becker *et al* 2020)	2020	Longitudinal FOV extension	Multi x-ray source
Tess (Reynolds *et al* 2022)	2021	Longitudinal FOV extension	Multi turn reverse helical trajectory

categorizes different studies according to different factors including main application, goal of the study, prior knowledge, trajectory parameterization, objective function and the optimization approach.
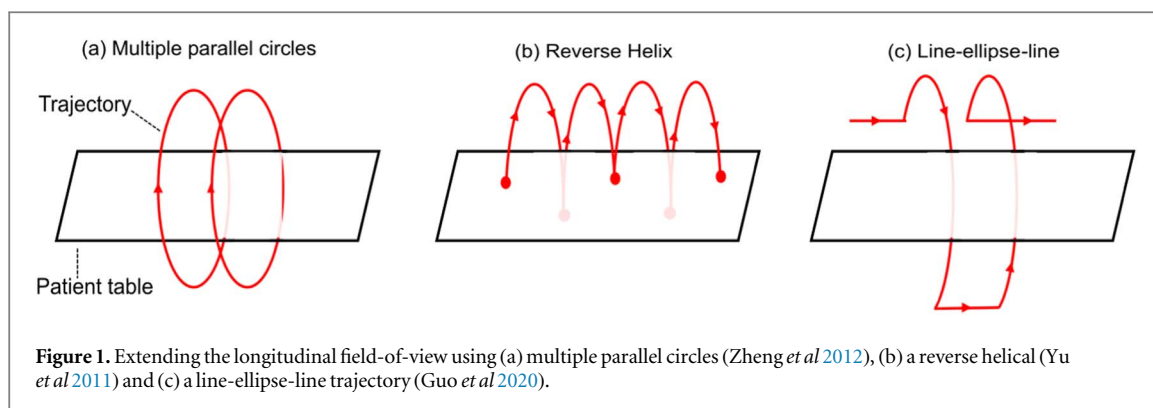
2.1. Extended FOV CBCT

A limiting factor for the continued expansion of CBCT imaging to new image-guided surgical procedures and radiation therapy treatments is the small FOV. In standard CBCT imaging, for example, the FOV is limited due to hardware design (i.e. detector length) and the predominate use of simple circular source-detector trajectories. Clinically, the limited FOV prevents long (e.g. head and neck, spine, and aorta) (Powell *et al* 2010, Kauffmann *et al* 2015, Richter *et al* 2015, Gang *et al* 2018, Boone *et al* 2019) and wide (e.g. pelvis, thorax, and liver) (Pung *et al* 2017) anatomical sites from being captured in a single CBCT image. Without modification to the hardware design, extended FOV CBCT imaging has been made possible by moving beyond the standard circular source-detector trajectory. Table 2 summarizes the proposed methods for CBCT FOV extension and helps to better illustrate the historical evolution of CBCT trajectory optimization with the goal of FOV extension.

2.1.1. Extending the lateral FOV

For image-guided surgery, extended lateral FOV imaging on robotic C-arm CBCTs has been solved by offset detector, rotated detector and dual isocenter approaches (Jaffray and Siewerdsen 2000, Jaffray *et al* 2002, Manhart *et al* 2010, Herbst *et al* 2015, Stromer *et al* 2016, 2016). In addition, extended lateral FOV imaging is already available through pre-programmed elliptical trajectories that take advantage of the flexibility of the system. The increase in lateral coverage, however, comes at the expense of longitudinal coverage. Comparatively for image-guided radiation therapy (IGRT), extended lateral FOV imaging using the on-board kV imager of a linac has been investigated theoretically with elliptical trajectories (Li *et al* 2010) and experimentally with trajectories such as multiple complementary circular scans (Yang *et al* 2014). In the complementary circular scan approach, Yang *et al* (2014) used two circular scans where the scans were offset in both the longitudinal and lateral directions from each other, enabling a total FOV with longitudinal coverage of 39.5 cm and lateral coverage of 45 cm. This is in comparison to the standard FOV (for a 40×30 cm^2 detector) with longitudinal coverage of 17 cm and lateral coverage of 25 cm and standard FOV with lateral offset with longitudinal coverage of 15.5 cm and lateral coverage of 45 cm. Ziehm mobile C-arm is a CBCT system which accomplishes its orbits through a series of shift and rotations which overcomes the limitations of a non-isocentric gantry.

2.1.2. Extending the longitudinal FOV

The conceptualization of non-circular source-detector trajectories, accompanied by specialized reconstruction algorithms for exact reconstruction, to facilitate extended longitudinal FOV CBCT imaging begun in the 1990s (Zeng and Gullberg 1992, Tam 1997). During the following two decades, as CBCT imaging systems became sufficiently sophisticated to implement alternative trajectories, three source-detector trajectories were identified

Figure 1. Extending the longitudinal field-of-view using (a) multiple parallel circles (Zheng *et al* 2012), (b) a reverse helical (Yu *et al* 2011) and (c) a line-ellipse-line trajectory (Guo *et al* 2020).

as leading candidates for realizing extended longitudinal FOV in clinical settings. These were multiple parallel circles (Kohler *et al* 2001, Zheng *et al* 2012, Gang *et al* 2018, Boone *et al* 2019, Mohamathu Rafic *et al* 2019), the reverse helical trajectory (Pearson *et al* 2010, Tan *et al* 2012, Yu *et al* 2015, Reynolds *et al* 2022) and the line-ellipse-line (Yu *et al* 2016, Guo *et al* 2020) (an extension of the circle-line-circle trajectory Lu *et al* 2012), as shown in figure 1.

Drawing inspiration from the established 'step-and-shoot' cine technique in CT, the multiple parallel circles represent the simplest modification of the standard circular source-detector trajectory (figure 1(a)). The first implementation of the multiple parallel circle trajectory clinically was in 2012 (Zheng *et al* 2012), using the on-board kV imager of a linac during IGRT for head and neck as well as prostate cancer. The trajectory contained two parallel circles separated by a longitudinal couch shift, ensuring minimal overlap of the individually reconstructed volumes, enabling an extension of the FOV from 15.9 to 31.8 cm (full-fan acquisition). Conceivably, increasing the number of circles would lead to further increases in the FOV. One advantage of the multiple parallel circle trajectory is being able to utilize standard filtered back projection reconstructions Feldkamp *et al* (1984), with no image acquisition occurring during the couch shift. Clinically, the disadvantages of the multiple parallel circle trajectory are the potential of doubling the imaging dose in the overlap region (especially if any organs at risk fall in the overlap) and possibility of reduction in geometric accuracy in the final combined image if the individual reconstructions are not rigidly registered. Once again turning to CT acquisitions for inspiration, the possibility of implementing helical trajectories on CBCT systems has also considered (Gupta *et al* 2006, Yu *et al* 2011, 2014, 2014). However, unlike CT systems where the gantry can continuously rotate, CBCT systems are typically limited to a finite rotation in one direction of between 240° and 400°. This requires the trajectory to take the form of a reverse helix, where the direction of the helix is reversed at the end of each rotation. The first experimental implementation of a reverse helical trajectory for extended longitudinal FOV CBCT imaging was conducted on a linac in 2012 (Tan *et al* 2012). As was the case for the multiple parallel circle trajectory, the application was again IGRT for both head and neck as well as prostate cancer. Tan *et al* (2012) combined simultaneous gantry rotation and table translation to complete the reverse helical trajectory and extend the FOV from 17 to 19 cm with a 360° helical scan, and out to 54 cm with a 720° helical scan. Soon thereafter in 2015 Yu *et al* (2016), the reverse helical trajectory was applied to image-guided surgery, enabling extended FOV in the interventional room. Taking advantage of the flexibility of robotic C-arm CBCT imaging systems, Yu *et al* (2016) designed their reverse helical trajectory to be solely realized by the movement of the C-arm (rotation and translation). This eliminated the need for precise couch control, which was and still is not universally available in all interventional rooms. Using a robotic C-arm CBCT imaging system and completing a total of 5 turns (240° per turn), Figure 1 (b), the reverse helical trajectory described by Yu *et al* enabled extension of the FOV from 16 to 27.4 cm. In 2021, Reynolds *et al* (2022) increased the angular coverage of each turn to 400° and re-introduced a continuous couch shift, allowing the FOV to be extended from 17 to 80 cm. Motivation to re-introduce the couch shift was driven by the limited space within an interventional room and the consideration of collision avoidance. Having the C-arm complete the entire trajectory (rotation and translation) requires the entire length of the extended FOV to be cleared from surgical equipment and/or personnel during the acquisition to avoid potential collisions. However, delegating the translation motion to the couch allows less clearance for the gantry rotation (i.e. that of a conventional circular source-detector trajectory). In pursuit of shorter acquisition times and simpler source-detector trajectories, efforts were placed into looking at including a line segment between rotational arcs (either elliptical Yu *et al* 2016 or circular Yu *et al* 2011, 2010) to extend the FOV (figure 1(b)). The first implementation of the line-ellipse-line trajectory on a robotic C-arm CBCT system was in 2020. Guo *et al* (2020) utilized two elliptical arcs separated by three line segments (line-ellipse-line-ellipse-line), enabling an extension of the FOV from 17 to 20 cm. Conceivably, increasing the number of ellipses and lines would lead to further increases in the FOV (figure 1(c)). Pivoting to hardware
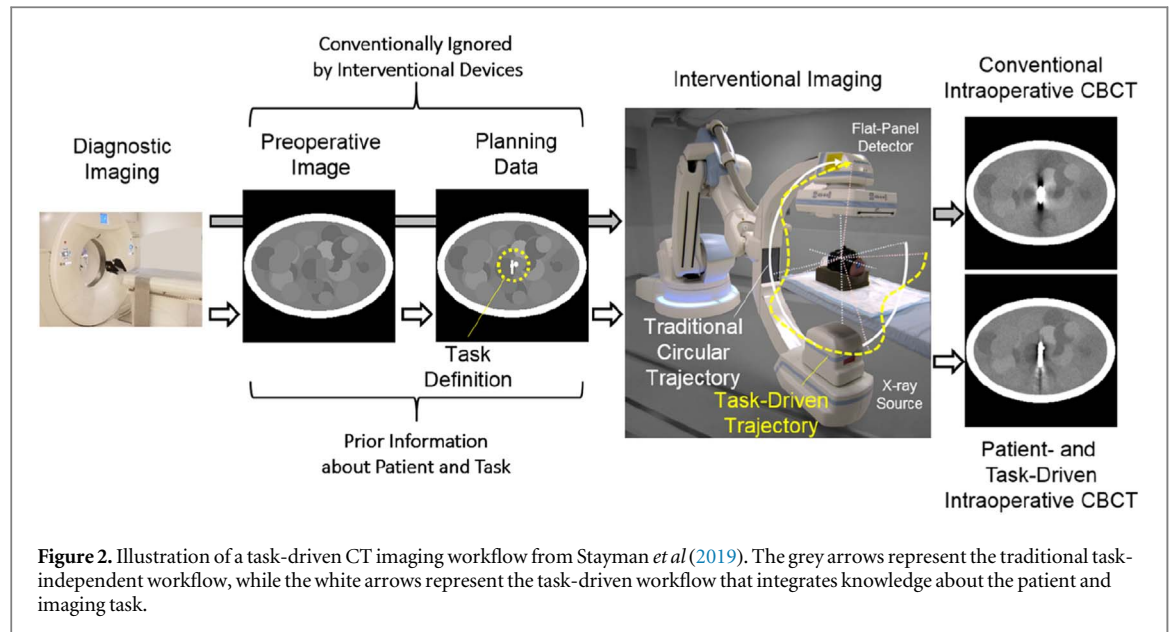
Figure 2. Illustration of a task-driven CT imaging workflow from Stayman *et al* (2019). The grey arrows represent the traditional task-independent workflow, while the white arrows represent the task-driven workflow that integrates knowledge about the patient and imaging task.

modifications, in 2018. Gang *et al* (2018) investigated the possibility of using 3 off-set sources, effectively enabling 3 parallel circular acquisitions simultaneously without the need for any translation. The focus of the work was on allowing long extremity sites to be captured in a single image, with the resulting FOV from this study, approximately 30 cm. In 2019, Boone *et al* (2019) looked to further expand the possible imaging geometries of CBCT systems, increasing the number of x-ray sources further as well as considering pulsing groups of the sources for cone beam and tomosynthesis applications (Becker *et al* 2020).
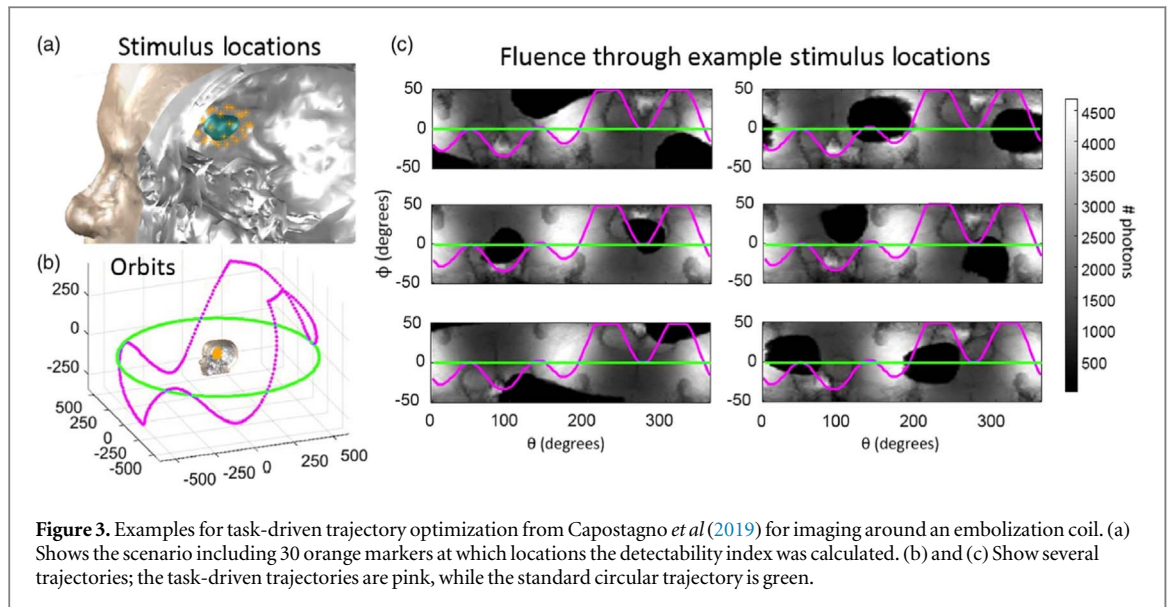
2.2. Task-driven CBCT trajectory optimization

CT scans are often performed to obtain the necessary information for a decision, either by a human or an automated algorithm. Examples are CT for interventional neuroradiology (Capostagno *et al* 2019), CT to guide screw placement (Yoo *et al* 2013), CT for bronchoscopy guidance (Setser *et al* 2020), weight-bearing CT (Maier *et al* 2011, Choi *et al* 2013, 2014) and CT for the guidance of complex needle paths (Busser *et al* 2013). In this context, a CT scan is ideal if it optimally increases the probability that the right decision is made. Figure 2 shows a workflow for task-driven imaging using a robotic C-arm CT system from Stayman *et al* (2019).

Let **H** be a task-function that corresponds to a crucial signal in the CT-scan, describing the location of interest and the frequencies of interest. Task-driven trajectory optimization aims to optimize the CT scan so that such tasks can be detected optimally. In contrast, task-driven trajectory optimization does not optimise the overall image quality of the CT scan. This means that the image quality of some features, e.g. image areas and even material transitions, can worsen, but the detectability of the specified task should be increased. Although task-driven CT scans therefore are ideal to analyze specific features with a small number of projections, they are not well suited to look for an unknown feature (Herl *et al* 2021).

To evaluate whether a CT assists in detecting a task, several options are available. Most obvious, experts, mainly doctors, can be asked directly in a so-called visual grading analysis (Verdun *et al* 2015). However, this is highly subjective and cannot be automated. Computational methods, so-called model observers can be applied to detect a task in a CT image automatically (Barrett *et al* 1993). Model observers can be described by a decision function $\lambda_{\text{Observer}}$ that maps the CT image to a probability number in [0,1] that depends on the probability that the task-signal is present in the image (Barrett *et al* 1993). The signal to noise ratio of a model observer, also called detectability index, indicates the performance of a model observer. The research groups of Siewerdsen and Stayman published several task-driven CBCT trajectory optimization approaches (Stayman and Siewerdsen 2013, Gang *et al* 2015, 2015, Stayman *et al* 2015, 2019). Gang *et al* (2011) showed that the so-called non-prewhitening matched filter observer (NPWMF) corresponds reasonably well to the human observer. Following (Verdun *et al* 2015), the detectability index of the NPWMF observer regarding a specific task **H** can be written in the Fourier-domain as:

$$d'^2_{\text{NPWMF}}(\Psi) := \frac{\left(\iiint [\text{MTF}_1(\Psi) \cdot \mathbf{H}]^2 \, df_x \, df_y \, df_z\right)^2}{\iiint \text{NPS}_1(\Psi) \cdot [\text{MTF}_1(\Psi) \cdot \mathbf{H}]^2 \, df_x \, df_y \, df_z}. \tag{1}$$

Figure 3. Examples for task-driven trajectory optimization from Capostagno *et al* (2019) for imaging around an embolization coil. (a) Shows the scenario including 30 orange markers at which locations the detectability index was calculated. (b) and (c) Show several trajectories; the task-driven trajectories are pink, while the standard circular trajectory is green.

With MTF_l and NPS_l denoting the local modulation transfer function (MTF) and the local noise power spectrum (NPS) at a location l and the integrals computed over the Nyquist region of (fx, fy, fz) spatial frequencies. Ψ generally denotes all available quantities of the image acquisition process, above all the projections.

For efficient calculation, Fessler (1996), Fessler and Rogers (1996) presented approximations for the MTF and the NPS when using the penalized-likelihood-reconstruction:

$$MTF_l(\Psi) := \frac{\mathcal{F}\{\mathbf{A}^\top \mathbf{D} \mathbf{A} e_1\}}{\mathcal{F}\{\mathbf{A}^\top \mathbf{D} \mathbf{A} e_1 + \beta R e_1\}}, \tag{2}$$

$$NPS_l(\Psi) := \frac{\mathcal{F}\{\mathbf{A}^\top \mathbf{D} \mathbf{A} e_1\}}{|\mathcal{F}\{\mathbf{A}^\top \mathbf{D} \mathbf{A} e_1 + \beta R, e_1\}|^2}. \tag{3}$$

With $\mathcal{F}$ denoting the 3D Fourier transform, A is the system matrix, D is a diagonal matrix of the projection values, e_1 is a unit vector indicating the relevant voxel at the location l, R is a regularization matrix of the penalized-likelihood-reconstruction and β is a weight for this regularization.

Stayman and Siewerdsen applied these approximations to use the detectability index of the NPWMF as a figure of merit for task-driven trajectory optimization for medical C-arm CT systems. In several approaches, they optimized trajectories using different parametrisation and optimization approaches. In Stayman and Siewerdsen (2013), Stayman and Siewerdsen optimized arbitrary sets of views on a spherical orbit using a greedy optimization approach. In Gang *et al* (2015), as part of a more general framework for CT parameter optimization, Gang *et al* applied the NPWMF for the optimization of task-specific circular trajectories using a gradient-based optimization approach. In Stayman *et al* (2015), Stayman *et al* optimized the tilt angle for every rotation angle using an evolutionary optimization algorithm, the CMA-ES Hansen and Kern (2004). In Stayman *et al* (2019), Stayman *et al* optimized trajectories based on compositions of basis functions by using B-Splines, again using CMA-ES (Hansen and Kern 2004) for optimization.

Capostagno *et al* (2019) demonstrated several examples for task-driven trajectory optimization following Stayman *et al* (2019) for interventional neuroradiology. They showed a reduction in noise and an increase of the detectability index ranging from 7% to 28%. As metal influence reduces the detectability, Capastagno *et al* showed that task-driven trajectory optimization is most efficient in the presence of highly attenuating components like metal. Figure 3 from Capostagno *et al* (2019) shows results for imaging an embolization coil using task-driven trajectory optimization.

Several other works built on the task-driven trajectory optimization frameworks of Stayman *et al* (2019, 2015). Zaech *et al* (2019) extended the approach for on-line trajectory optimization. Fischer *et al* (2016) applied and extended the approach for industrial CT (see chapter 3)

2.3. CBCT artifact reduction

CBCT presents many image quality factors; however, cone-beam sampling effects are among the most challenging to assess in a rigorous, quantitative manner since they are highly object-dependent. Tuy's sufficiency condition (Tuy 1983) states that, for a known and fixed source trajectory, any plane through a point in the target object must intersect the source trajectory to be precisely reconstructed. Tuy defines the requirements for complete image sampling and, therefore, a theoretically accurate image reconstruction by identifying the points

Figure 4. Illustration of the three-source Carestream CBCT scanner installed at Imaging for Surgery, Therapy and Radiology (I-STAR) laboratory, Johns Hopkins University. Upper, Middle and Lower denote the upper, middle, and lower x-ray sources, respectively.

in the FOV that can be reliably reconstructed. In the scenario of a circular source trajectory, no point outside the trajectory plane is fully sampled (in terms of the Tuy's condition). Various approaches with diverse source-detector geometries such as the OnSight 3D Extremity CT System (Carestream Health, Rochester, NY, USA) Gang *et al* (2018) featuring three pulsed sources and the multi-source IZOview breast CT System (Izotropic Corporation, BC, Canada) Boone *et al* (2019), with multiple simultaneously pulsed sources, as well as non-circular scan trajectories allow improving data completeness. Nevertheless, these more complex systems and configurations reveal the need for quantitative and practical image quality metrics that are not limited to the axial plane. A new figure of merit for sampling completeness ($\tan(\Psi)_{min}$) has been proposed (Tersol *et al* 2022) to analytically quantify cone-beam artifact using a three-source CBCT scanner (figure 4), where for every point in the FOV, Ψ_{min} represents the minimum ray angle it generates with the source across the scan trajectory. Effectively, $\tan(\Psi)_{min}$ defines to what extent the Tuy's condition is met for any point in the FOV and is a function of the scan trajectory and the relative position of the point in the test object with the source. By means of the Corgi Phantom Siewerdsen *et al* (2019), which contains a series of disk-pairs distributed across the *z*-axis and parallel to a circular non-tilted scan trajectory (i.e. the axial plane), the magnitude of the artifact was computed from the modulation in longitudinal signal profiles across the disk pairs. The higher the modulation, the lower the artifact. The relationship between $\tan(\Psi)_{min}$ and the modulation was continuous and consistent across all experiments performed, proving the connection between this analytical FOV and the empirical measurements and establishing $\tan(\Psi)_{min}$ which is an easy computable metric that provides valuable insight on sampling completeness Tersol *et al* (2022). In addition, the work Tersol *et al* (2022) illustrated the advantages of tilted source-detector trajectories, which displayed an evidently improved modulation between the disks, proving that for C-arm tilts between 0°and 15°, the modulation range decreased significantly with an increase in the tilt.

The authors in Carrino *et al* (2014) performed an initial assessment of dose and the image quality of a CBCT scanner including 3 sources along the *z*-direction used to extremity imaging (including the weight-bearing lower extremities). They reported that a dedicated extremity CBCT scanner (e.g. scanner shown in figure 4) which is able to image upper and lower extremities (including weight-bearing examinations) can provide satisfactory dose characteristics and an adequate image quality and less artifact which can be used for further evaluation in clinical applications. In another study Zbijewski *et al* (2011), authors evaluated the design and initial imaging performance of a CBCT system used for musculoskeletal (MSK) extremities. Their proposed design complements conventional CT and MR and showed that a variety of potential clinical scenarios e.g. diagnosis, assessment of therapy and treatment planning can benefit from their approach. They used a theoretical modeling including cascaded systems analysis of MTF as well as detective quantum efficiency which was computed as a function of dose, source power, kVp, system geometry and filtration. Their results demonstrated that their proposed system can deliver volumetric images of the extremities including soft-tissue contrast resolution which is comparable to diagnostic CT. In addition, their system can improve the spatial resolution and reduce image artifact at potentially reduced dose. In another study Demehri *et al* (2014), the same research group evaluated visualization tasks using CBCT imaging in comparison to multi-detector CT (MDCT) for musculoskeletal extremity imaging. Ten cadaveric hands and ten knees were used to assess soft tissue and bone visualization tasks using a clinical MDCT and a dedicated CBCT prototype using nominal protocols (120 kV p–300 mAs for MDCT; 80 kVp–108 mAs for CBCT). Their results showed the CBCT could lead to an excellent
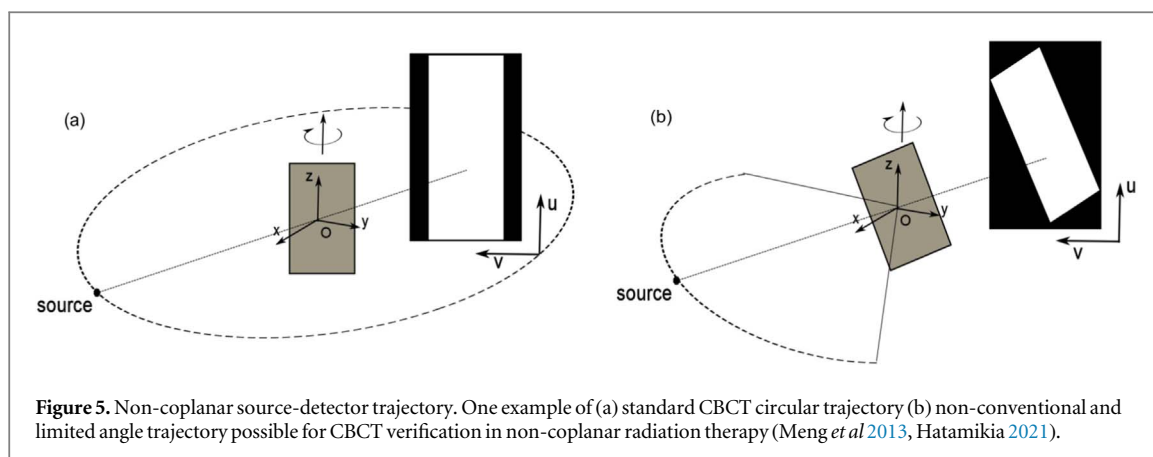
Figure 5. Non-coplanar source-detector trajectory. One example of (a) standard CBCT circular trajectory (b) non-conventional and limited angle trajectory possible for CBCT verification in non-coplanar radiation therapy (Meng *et al* 2013, Hatamikia 2021).

image quality in visualization of bone visualization and satisfactory image quality in visualization of the soft tissue.

2.4. Collision avoidance trajectory optimization and angular range reduction

One limitation regarding the conventional circular CBCT trajectory is the wide angular range which is needed for reconstructing the 3D object (either full circle (360°) or short circle (180°+fan arcs)). However, there are very often clinical scenarios e.g. during surgery where only a small projection set with a limited angular range can be acquired. The number and the nature of the assistant tools imposes restrictions on the available space in the intervention room. In these cases, the standard circular trajectory is not realizable without rearranging the surgical equipment and/or personnel. Several clinical applications have found the angular range less than 180° beneficial (Sidky *et al* 2009, Je *et al* 2014, Hatamikia *et al* 2020). In addition to the interfering equipment, the patient size can also impose such challenges specially in complex interventions where repetitive 3D scans are needed and other medical devices hamper access to the patient; therefore, such a circular trajectory with wide angular range can be problematic due to the device collisions, patient positioning and the operation room setup by itself (Ladikos *et al* 2008, Padilla *et al* 2015, Hua *et al* 2017, Mann *et al* 2019).

Two examples of possible kinematic constraints due to the patient size and other medical devices are illustrated on the C-arm geometry in figure 5. Alternative data acquisition trajectories can assist actuating the CBCT system around any interfering structure and therefore limited angle collision-avoidance source-detector trajectories are of great potential advantage for kinematically challenging clinical scenarios. Several collision detection techniques have been researched for radiotherapy in different forms including 3D or computer-aided design (CAD) design systems (Humm *et al* 1995, Zou *et al* 2012, Yu *et al* 2015) or using optical detection approach based on the laser camera (Brahme *et al* 2008). In a recent study Davis *et al* (2019) authors proposed to modify the source-detector trajectories to address the collision problem in radiotherapy. They investigated trajectories for CBCT imaging in IGRT which are able to avoid collisions which happen mostly between the gantry, kV detector and the patient due to the patient size, pose or fixation devices. They proposed to use a virtual isocenter with an adjustable magnification during the data acquisition while keeping the image quality comparable with conventional imaging. In their proposed method, a virtual isocenter trajectory moves constantly the patient while gantry rotation preserves the separation between these two. In their strategy, the kV detector supported a dynamic movement and magnification which helped to avoid the angular range with the potential collisions while recording sufficient data to preserve required FOV. Their proposed technique of collision avoiding trajectories could successfully avoid patient-device collisions while resulting in an image quality comparable to the standard circular trajectory and therefore enabling CBCT imaging for those patients who cannot otherwise be imaged.

In another study Zhao *et al* (2019) scan orbits and acquisition protocols were optimized for 3D imaging of the weight-bearing spine using a Multitom Rax system (twin-robotic x-ray system). The authors proposed a simulation framework which can be used for systematic optimization of protocols in terms of imaging dose, noise, scatter and task-based performance in 3D image reconstructions. In addition their proposed trajectories using the Rax system has a large flexibility to prevent patient collisions.

Non-coplanar radiation therapy is another clinical application where limited angle source-detector trajectories can be of potential advantage. Non-coplanar beams are crucial in treatment of cranial/non-cranial tumors. However, treatment verification using CBCT is usually challenging due to the patient couch rotation/ kicks. The reason is that usually limited and unconventional angles are possible in order to prevent collisions between gantry, patient, on-board imaging system and couch (Meng *et al* 2013, Padilla *et al* 2015). In such cases,
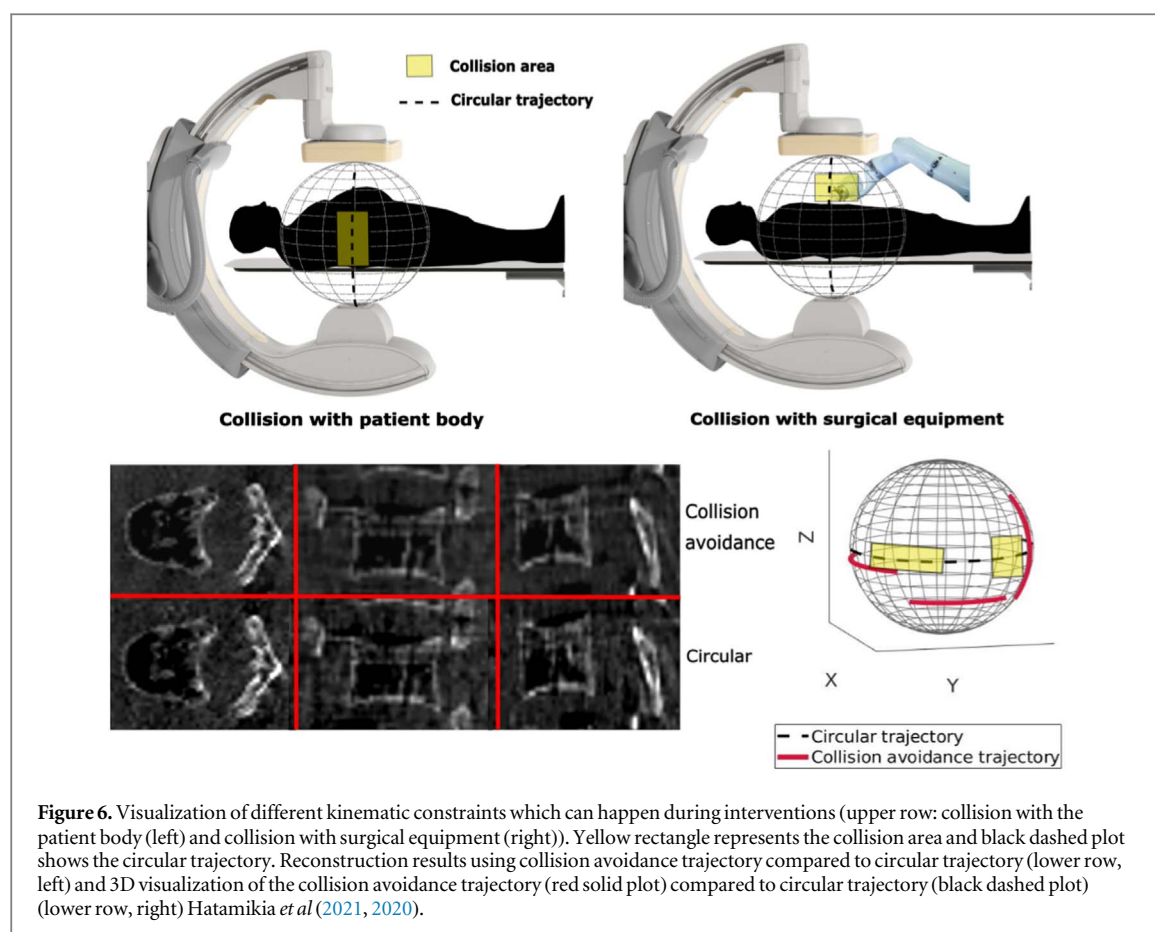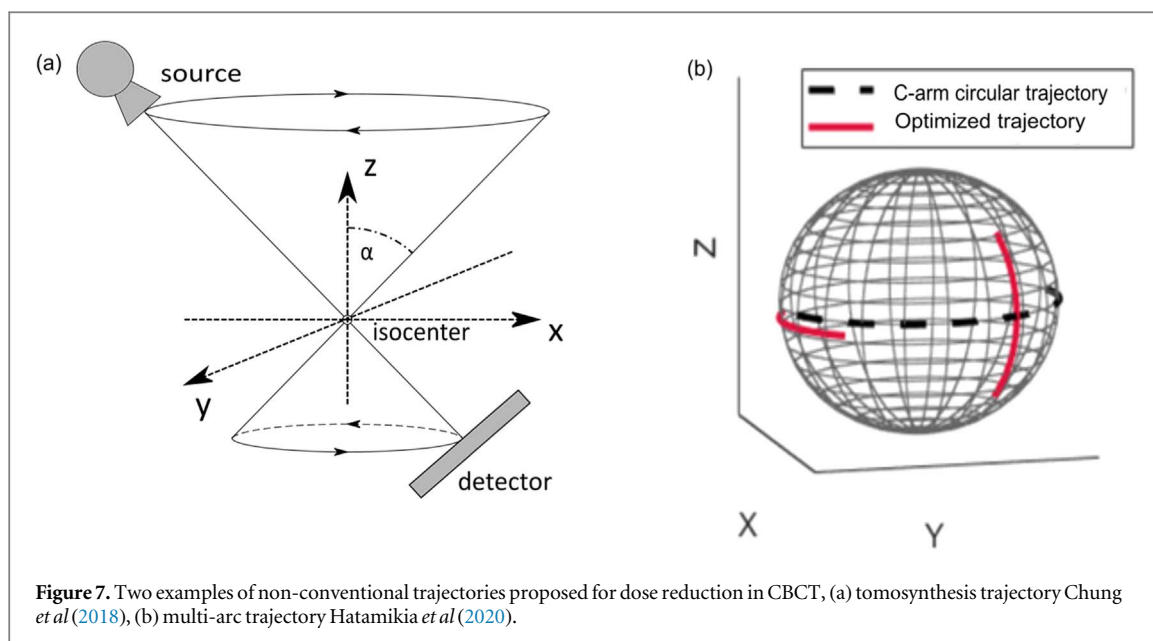
Figure 6. Visualization of different kinematic constraints which can happen during interventions (upper row: collision with the patient body (left) and collision with surgical equipment (right)). Yellow rectangle represents the collision area and black dashed plot shows the circular trajectory. Reconstruction results using collision avoidance trajectory compared to circular trajectory (lower row, left) and 3D visualization of the collision avoidance trajectory (red solid plot) compared to circular trajectory (black dashed plot) (lower row, right) Hatamikia *et al* (2021, 2020).

source-detector trajectory with a limited angular range is required. Meng *et al* (2013) suggested a CBCT verification strategy which combines a prior image constrained compressed sensing (PICCS) reconstruction method with the image registration step. They used a pre-existing CT or CBCT at the normal position. The translated and rotated prior image according to the small patient table and translation was served as the initial image for PICCS reconstruction. Their results showed that using their approach efficient reconstructed images from the patient can be reconstructed using projection sets with an angular range of 60°. They showed that they can appropriately verify non-coplanar beams using the CBCT scans with patient table rotations of 45°(figure 5).

Hatamikia *et al* (2020, 2021) proposed a framework for target-based trajectory design in CBCT imaging. They designed collision avoidance source-detector trajectories which could enable CBCT imaging under kinematic constraints for cases where standard circular trajectories are not feasible. They defined two different types of rotation: (1) right anterior oblique (RAO)/left anterior oblique (LAO) rotation while having an oblique at various fixed cranial (CRA)/caudal (CAU) angles, (2) CRA/CAU rotation with an oblique at various fixed RAO/LAO angles. Each of these possible rotations were divided into subsets of short arcs (figure 5). This approach allowed for additional degrees of freedom as compared to a limited view single arc as it allows for increased flexibility under inevitable kinematic constraints and facilitated CBCT under severe kinematic constraints, for instance when arcs larger than 80°are not feasible. In addition, it provides flexibility which could enhance reconstruction compared to a continuous limited view single arc. The Feature SIMilarity Index (FSIM) was used as the objective function in order to evaluate the imaging quality provided by different novel trajectories. They showed that their proposed optimized trajectories which included three short arcs could achieve an image quality comparable to that of the standard circular CBCT for different anatomical targets. Considering the fact that their proposed trajectories were designed under strong kinematic constraints, the achieved performance was significant (figure 6).

2.5. Dose reduction

The number of projections which are required to reconstruct an adequate CBCT image using a circular source-detector trajectory is high and introduces a considerable radiation dose delivered to the patient. Recently, the accumulated radiation dose due to the repetitive use of CBCT scans needed for image-guided procedures as well as daily pretreatment patient alignment for radiation therapy has become a concern. Therefore, it is desirable for patient and health care providers to reduce the amount of radiation exposure required for these procedures.

Figure 7. Two examples of non-conventional trajectories proposed for dose reduction in CBCT, (a) tomosynthesis trajectory Chung *et al* (2018), (b) multi-arc trajectory Hatamikia *et al* (2020).

There are several studies which have evaluated the radiation dose from CBCT for interventional procedures. Authors in Stock *et al* (2012) reported that although the radiation dose from a single CBCT scan compared to the treatment dose is negligible, the accumulated CBCT dose received by patient during the entire radiotherapy sessions can be significantly higher, therefore a careful dose management is required. Another research group reported Berris *et al* (2013) that in some cases C-arm CBCT delivers a comparatively high dose to patients and the total delivered radiation dose can reach or even exceed the dose from a corresponding MDCT protocol. Different approaches have been proposed in order to perform a CBCT dose reduction by means of filters e.g. copper or bowtie filters (Roxby *et al* 2009, Sun *et al* 2017), optimizing scan parameters (Wang *et al* 2008, Abul-Kasim *et al* 2012), using statistical reconstruction (Wang *et al* 2014, Sohn *et al* 2020) and projection reduction (Lu *et al* 2010). The authors in Lu *et al* (2010) investigated the effect of projection reduction on image registration accuracy and image quality for CBCT reconstruction. In another study Sun *et al* (2017) authors evaluated the breast dose using routine thoracic CBCT and investigated the possible dose reduction protocols. They tried to reduce the exposure dose by means of partial arc with bowtie filter and investigated the effect of this dose reduction method on image registration accuracy. The dose received by breast for variety of scanning protocols and also for different breast sizes was compared. They concluded that using 220°partial CBCT arc scan with bowtie filter a significantly lower dose could be received by contralateral breast while the accuracy of the image registration was not reduced. Recently, the advent of advanced robotic C-arms for clinical usage has prompted researcher to assess dose reduction possibilities by means of modifying imaging scan trajectories. A full 3D CBCT data set is not necessary to acquire for certain medical applications and only specific information such as the position of high-contrast objects or particular lesion is relevant. In diagnostics, tomosynthesis can offer tomosynthesis specific scanning protocols for such applications (Stevens *et al* 2003, Nett *et al* 2007, Claus *et al* 2015, Chung *et al* 2018). Although such scans offer less image quality compared to standard CBCT, they provide the critical information at lower dose exposures for diagnosis applications. This can be helpful for interventional tasks such as angiography, seed position checking or catheter tracking where only selective information is essential. Therefore, the integration of tomosynthesis methods in interventional radiology would offer a new approach to reduce the dose exposure in imaging. Chung *et al* implemented a circular tomosynthesis orbit (figure 7(a)) on a clinical CBCT system using a step-and-shoot technique (Chung *et al* 2018). Although limited angular artifacts were observed in the reconstructed images, they concluded that circular tomosynthesis scans can help to reduce the dose exposure when only the positions of high-contrast objects need to be determined. In Hatamikia *et al* (2020, 2020) authors proposed a new approach for dose reduction in CBCT by personalizing scan trajectories. The basic idea was to design trajectories which include only the most informative projections with arbitrary 3D orientation while skipping unnecessary projection data in order to reconstruct individual VOIs. They proposed customized multi-arc trajectories for C-arm CBCT reconstruction. A VOI was selected from a prior diagnostic CT scan, and a variety of possible trajectory combinations from short arcs was simulated and reconstructed. The optimal arc combination is selected through maximizing an objective function fed by the imaging quality within a VOI provided by different x-ray positions on the digital phantom (prior CT). Using this approach, they could achieve a reasonable image quality compared to the reference C-arm circular CBCT for different VOIs inside an anthropomorphic phantom while reducing projections to a fourth of
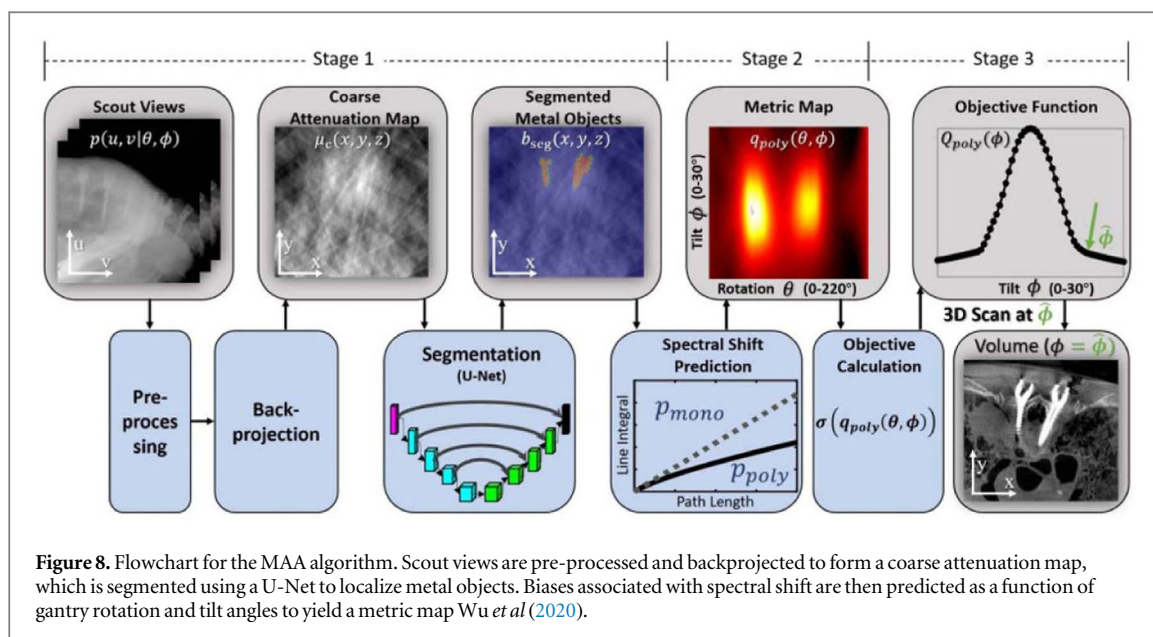
Figure 8. Flowchart for the MAA algorithm. Scout views are pre-processed and backprojected to form a coarse attenuation map, which is segmented using a U-Net to localize metal objects. Biases associated with spectral shift are then predicted as a function of gantry rotation and tilt angles to yield a metric map Wu *et al* (2020).

a standard circular scan. The lower number of projections makes their proposed multi-arc trajectories suitable for low-dose CBCT interventions. They also showed their proposed trajectories could improve the reconstruction performance in the VOI with respect to circular trajectories with equivalent angular sampling (figure 7(b)).

2.6. Metal artifact reduction

Non-conventional trajectories as described in section 2.3 can help facilitating CBCT under kinematic constraints; however, even in case with adequate actuation space where imaging with the standard circular trajectory is feasible, a suboptimal location of the imaging target adjacent to metal implants, needles, surgical tools or other radiopaque structures such as bones can result in insufficient image quality in the reconstructed CBCT image (Wu *et al* 2020). Deterioration of the image quality—which originates from metal artifacts and radiopaque structures for instance—arises from a bias and/or discrepancy between the assumed model for reconstruction of the projections (i.e. the inverse model) and the actual physical processes of image formation (i.e. the forward model) Boas and Fleischmann (2012). Non-circular orbits can be used in some cases to avoid non-beneficial projections and therefore improve image quality in vicinity of the metal objects substantially Gang *et al* (2020). The authors in Thies *et al* (2020) tried to perform orbit optimization on-the-fly in order to improve reconstruction image quality in the presence of metal artifacts. They proposed to optimize the C-arm CBCT source-detector trajectory during the CBCT scan to improve reconstruction image quality in the vicinity of metal artifacts. They performed the adjustments during the scan using a Convolutional Neural Network (CNN) and regressed an image quality metric over all possible next projections given the current x-ray image. Adjusting the scan trajectory to obtain the optimal views resulted in non-circular source orbits that could avoid poor images and improved image quality mainly in terms of metal artifacts. A method in order to reduce the impact of metal artifacts by prospectively defining C-arm source-detector orbits was proposed in Wu *et al* (2020) (figure 8). Their proposed metal artifact avoidance (MAA) method could mitigate metal-induced biases in the projection data and does not need exact prior information of the patient or metal implants. The MAA method included coarse localization of metal objects, model-based estimate of metal-induced x-ray spectral shift for possible source-detector trajectories and identification of an optimized orbit in order to reduce the variation in spectral shift. Their metal-avoidance orbits could reduce root-mean-square error (RMSE) in the reconstructed image and 'blooming' artifacts by 46%–70% and 20%–45% respectively.

In Gang *et al* (2020), Maier *et al* (2015) the authors used non-circular trajectories to maximize data completeness in the presence of metal. They used a local data completeness metric based on Tuy's condition. Their measure counts the percentage of great circles which are sampled by an individual trajectory, accounts for the presence of metal object and tries to make use of x-rays that pass through the target object but avoid x-rays that pass through the metal object. The performance of sinusoidal orbits at different frequencies and magnitudes in metal artifact reduction was investigated. They compared their results with circular and tilted circular trajectories and they observed that a sinusoidal orbit of two cycles per rotation can perform better in removing metal artifacts. In another study using the same image quality metric Gang *et al* (2020), the authors tried to optimize non-circular orbits in simulations with the aim of maximizing Tuy's condition in the presence of metal
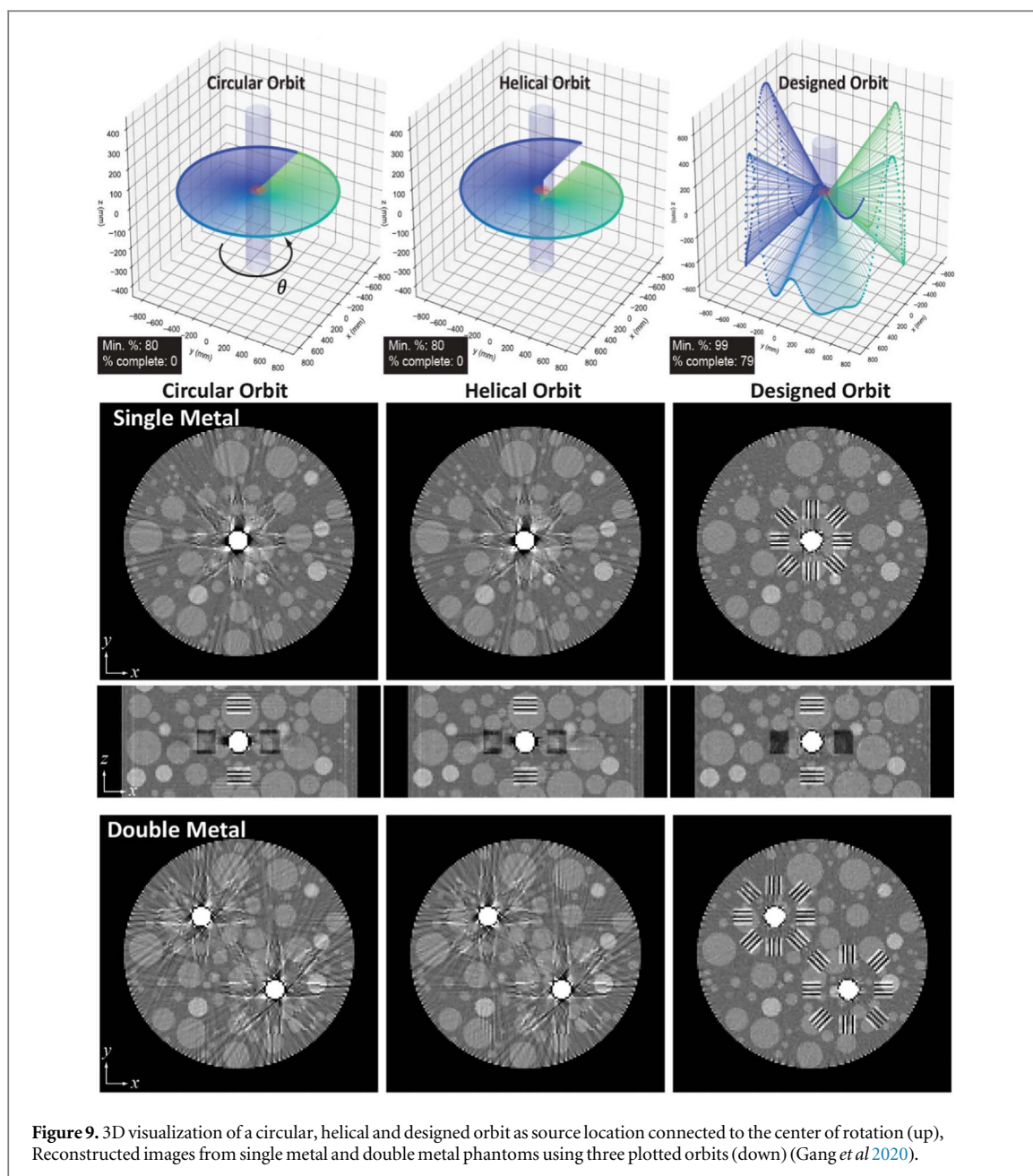
Figure 9. 3D visualization of a circular, helical and designed orbit as source location connected to the center of rotation (up), Reconstructed images from single metal and double metal phantoms using three plotted orbits (down) (Gang *et al* 2020).

objects (figure 9). Their optimized orbits showed a great improvement in metal artifacts reduction and visibility of in-plane structures which would be obscured by metal object. Their proposed orbital design scheme tried to optimize trajectories over arbitrary metal locations and therefore, the optimized arbitrary trajectory was generally useful regardless of where metal object is located. In addition, their approach was resilience also in case of having multiple metal objects. In a recent study Hatamikia *et al* (2022), the performance of the prior image constrained compressed sensing (PICCS) CBCT reconstruction in combination with optimized source-detector trajectories in presence of a needle inside an anthropomorphic thorax phantom was evaluated for cases where an initial standard CBCT is a available. Their results using small projection set demonstrated a significant reduction in metal artifacts and improvement in needle localization compared to the FDK and PICCS methods when using a sparse-view circular trajectory.

3. Trajectory optimization in industrial CBCT

CBCT is also relevant for industrial applications (Zabler *et al* 2021), especially in materials research and quality control. A high variety of objects is examined. In some cases, examined objects are made from only one material, e.g. plastic or metal. In other cases, examined objects consist of many components of different materials and sizes.
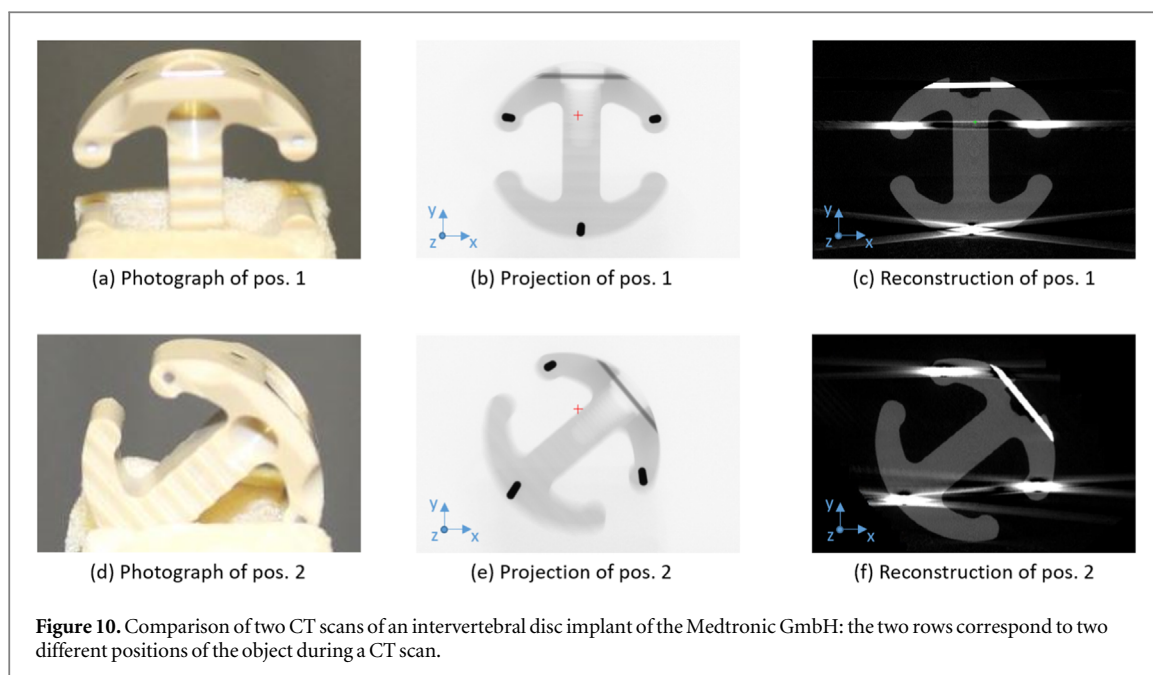
Figure 10. Comparison of two CT scans of an intervertebral disc implant of the Medtronic GmbH: the two rows correspond to two different positions of the object during a CT scan.

In principle, trajectory optimization in industry is equally relevant and follows the same basic steps as in medicine. As many relevant objects contain metal or are made completely of metal, artefact reduction and image quality improvement is crucial for many applications. Dose reduction is not necessary as x-rays do not harm objects. Nevertheless, a reduction of the projection number is beneficial to reduce the scan time and the cost of the scan.

Analogous to medicine, in most industrial trajectory optimization approaches, the source-object-distance and the source-detector-distance is assumed to be constant. In a standard industrial CBCT system, an object is placed on a turntable between the x-ray source and the x-ray detector. By rotating the object, projections are generated from a circular trajectory. In this case, the optimization of such circular trajectories is performed by optimizing the object position on the turntable. In order to demonstrate the influence of the object position regarding image quality and metal artefacts, figure 10 shows two CT scans of the same object, but with different object positions. In both cases, metal artefacts appear in front of and behind metal components. However, due to the rotation, different regions of the object are disturbed by metal artefacts.

With standard industrial CBCT systems, objects of up to 40 cm maximal diameter can be scanned. To scan large-scale objects, e.g. automobiles, non-standard systems like robot-supported CBCT systems are required. In industrial twin robotic CBCT systems, the source and the detector are mounted on two separate robots that can move freely around the object. This allows for arbitrary scanning trajectories, limited only by the range and flexibility of the robots and the size and shape of the object. Figure 11 shows an industrial twin-robotic CBCT system.

In the following, first, trajectory optimization approaches for standard industrial CBCT system for circular trajectories and, second, trajectory optimization approaches for twin robotic CBCT systems for arbitrary trajectories are reviewed.

3.1. Object position optimization in standard industrial CBCT

Amirkhanov *et al* (2010) used CAD data of the object in form of an STL (Standard Triangle/Tessellation Language) file as the prior knowledge. They optimized the object position of mono material objects with the aim of optimally digitising the surface of the object given by this STL file. They used a brute force approach utilizing three figures of merit. First, for each position the maximum and the average penetration lengths of the relevant x-rays were considered. High penetration lengths led to higher probability and strength of artefacts and image quality issues like beam hardening, noise and metal artefacts and, thus, were minimized. Second, for each of the surface triangles, they considered its representation in the Radon space. If x-rays parallel to a surface triangle have been measured, the necessary information for imaging the corresponding surface has been acquired. To ensure true reconstruction of most surfaces, the amount of surfaces for which parallel x-rays are measured is maximized. Additionally, a metric for the object stability is considered. Using these three metrics, a brute force approach was applied for finding the optimal object position.

Figure 11. Twin robotic CT system of the Deggendorf Institute of Technology at the Technology Campus Plattling.

Ametova *et al* (2017) and Butzhammer *et al* (2020) examined the concept of analyzing the measurements according to each surface triangle for further object position optimisation. Reisinger *et al* (2011) and Schmitt *et al* (2012) both analyzed the penetration lengths for object position optimization.

Schielein *et al* (2016) and Xue and Suzuki (2017) optimized object positions for scans with optimal image quality for complete objects. Based on reconstructions of simulated projections as prior knowledge, they applied brute force using the Shannon entropy (Shannon 1949) as the objective function. In most industrial CBCT scans, objects consists of a small amount of homogeneous materials like plastic or metal. Therefore the histogram of reconstructed volumes should contain only a few values with high numbers and many values close to zero. The Shannon entropy, a concept of information theory, is utilized to analyze the histogram accordingly.

Grozmani *et al* (2019) optimized object positions for scans with optimal image quality for complete objects. They used simulated projections as the prior khowledge and applied a brute force approach for the optimization. In Buratti *et al* (2016), Buratti presented a method to the contrast-to-noise-ratio (CNR) in the reconstructed volume based on the ratio of the initial intensity and the measured intensity at the detector. Grozmani *et al* utilized this estimation to choose the object position for optimizing the expected CNR of the resulting reconstruction.
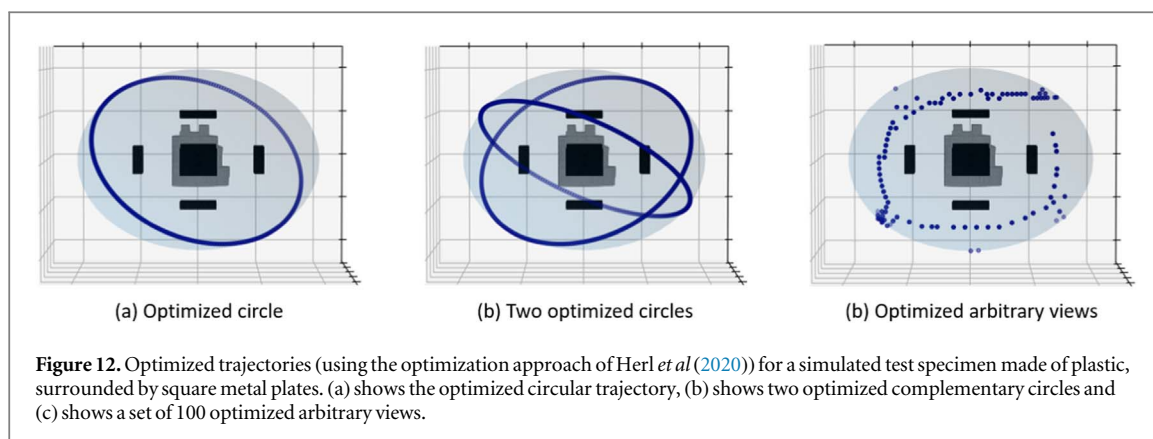
3.2. Optimization of arbitrary trajectories for industrial twin robotic CBCT

To optimally detect defects in two-dimensional projections without reconstruction, Brierley *et al* (2018) used CAD data as well as the type of the defect, i.e. shape and size of expected defects as prior knowledge. After simulating projections of the examined object with and without the defect, they analyzed the CNR of the difference of both projections, i.e. the influence of the defect. Maximising this CNR, the best views were chosen using were chosen using Genetic algorithm as the optimization method (Jones 2006).

For optimization of the image quality of specific tasks, mainly specific object surfaces, Fischer *et al* (2016) extended the approach of Stayman *et al* (2015) (see section 2.2) to industrial CT applications, based on simulated projections from CAD data. Using the detectability index of the non-prewhitening model observer as object function, they optimize arbitrary views using a greedy optimization approach.

For the reduction of scan time while ensuring task-based image quality, Bauer *et al* (2020) analysed the Fourier transform of the reconstructed volumes using simulated projections from CAD data. Based on the assumption that the Fourier coefficients should be sparse, they optimized arbitrary views using a brute force approach.

Herl *et al* optimized sets of arbitrary views based on data completeness conditions (Herl *et al* 2020, 2021). Tuy presented necessary conditions for trajectories that ensure true reconstruction (Tuy 1983). However, the so-called Tuy conditions only work for continuous curves, i.e. continuous trajectories. Herl *et al* extended the Tuy conditions, to generate metrics for the data completeness of sets of arbitrary views that do not have to share a continuous curve. Using these metrics as figures of merit, Herl *et al* optimized CT trajectories for several different scenarios. For standard industrial CBCT systems, they optimized circular trajectories and complementary circles for multipositional data fusion Herl *et al* (2018, 2019) using brute force optimization. For twin-robotic CBCT systems, they optimised arbitrary sets of views by iteratively choosing the views that optimally increased these metrics for provided regions of interest. By excluding x-rays that are corrupted due to

Figure 12. Optimized trajectories (using the optimization approach of Herl *et al* (2020)) for a simulated test specimen made of plastic, surrounded by square metal plates. (a) shows the optimized circular trajectory, (b) shows two optimized complementary circles and (c) shows a set of 100 optimized arbitrary views.

metal influence, the approach of Herl *et al* can be applied to find trajectories that reduce metal artefacts. Figure 12 shows optimized trajectories for different scenarios for a simulated multi-material test specimen.

In Herl *et al* (2021), Herl *et al* presented a trajectory optimization approach that jointly applied these data completeness metrics and the detectability index of the NPWMF, following Stayman *et al* (2019) (see section 2.2). Thereby they created a trajectory optimization approach that can be fine-tuned to optimize task-dependently, task-independently or a combination of both.

4. Discussion

CBCT imaging is widely used in image-guided therapy e.g. image-guided surgery and image-guided radiation therapy. In image-guided interventions, the CBCT systems which are installed on portable C-arms are highly flexible imaging options and significantly support minimally invasive surgeries which are conducted increasingly with robotic assistance in the modern, hybrid intervention rooms. The potential for improved CBCT image quality via non-circular orbits was recognized in early work on cone-beam reconstruction. While the conventional CBCT imaging neglects the benefit of prior knowledge in the image acquisition process, the proposed trajectory optimization techniques in the last decade leverages the wealth of available information and combines it with advanced methods to perform a target-based reconstruction. Therefore, the existing information in interventional imaging is fundamentally integrated into the image acquisition process. This makes the imaging systems more aware of the objects and imaging tasks which are intended to be imaged and therefore can lead to an increased imaging performance and potential reduction in dose. Another important advantage of this approach is the possibility of 3D imaging under severe kinematic constraints, which can be achieved by modifying the scan geometry taking into account any available spatial constraints due to patient size or other medical devices. So far, the proposed collision avoidance trajectories only included optimizing angulation; by means of flexible imaging platforms such as a robotic C-arms, additional degrees of freedom, for example translation of the source and/or detector, can also be incorporated which can provide more flexibility and access and also potentially better imaging performance. One other recent application in which non-conventional CBCT trajectories are to be of most benefit is the reconstruction in presence of metal objects. Task-driven orbits were demonstrated to significantly improve strong metal artifacts and strong streaks which confound visualization of nearby, low-contrast structures. This is a common problem in image-guided interventions where CBCT images which are taken during the interventions often include metal objects, and the regions of interest tend to be in vicinity to such metal instrumentation.

Over the last decade, there has been constant efforts to formulate sophisticated objective functions to solve the orbit optimization problem. In order to optimize data acquisition, cascaded systems analysis as well as approximations of local noise and spatial resolution have been utilized to calculate the detectability index of tomosynthesis and task-aware orbits. The detectability index integrates knowledge on the imaging task as well as the spatial-frequency dependent transfer of the noise and spatial resolution. It is generally accepted that the use of these measures provides an ideal definition of the imaging performance. However, such computations are very time consuming and there is usually the immediate need, for an optimization algorithm to be able to accommodate the strict time restrictions of intra-interventional implementation and therefore online trajectory optimization is a particularly valuable tool. There were recent efforts to perform orbit optimizations on-the-fly in order to reduce metal artifacts by means of leveraging CNN rapidity to predict the next best view angle as well enabling an online CBCT imaging under kinematic constraints by combining multiple arc trajectories. However, there are still several challenges; for instance, online geometric calibration is needed to be addressed to enable the online trajectory optimization approach in order to fulfill the level of accuracy and robustness needed

for clinical applications. Although such a geometric calibration is very challenging, several practical solutions have been already proposed in the literature in order to address this problem. Wu *et al* (2020) showed a library of geometric calibrations can be interpolated to give reasonable calibration of an arbitrary non-circular orbit. Another study by Capostango *et al* (2016) solved such calibration problem for CBCT imaging using a 2D/3D registration approach. In another study Jacobson *et al* (2018) the authors proposed a calibration approach using an array of line-shaped, radio-opaque wire segments. The geometric parameter estimation could be accomplished by means of relating the 3D line equations which is a representation of the wires to the 2D line equations related to their projections. Their approach based on line fiducials could simplify many challenges regarding fiducial recognition as well as extraction in an orbit-independent manner.

Aside from the optimization prospective of the orbit geometry before or during intervention, the subsequent reconstruction of the projections acquired using the non-circular trajectory remains a challenge. Typically, reconstruction algorithms for non-circular trajectory data have relied on both model-based and analytical techniques. Theories for exact solutions exist for explicit classes of non-circular orbits; some are a kind of filtered back projection or differentiated back projection—including a subsequent inverse Hilbert transform in the image domain. However, for an exact reconstruction of a region of interest, there is the general requirement for that region to be covered in so-called R-lines; consequently, analysis of R-line coverage is necessary when investigating new source trajectories (Pack *et al* 2005, Yu *et al* 2011). As an alternative, model-based iterative reconstruction (MBIR) techniques can be applied to arbitrary trajectory data without requirement for adaptions; MBIR technique then provides a general best-estimate based on the available data as it can integrate knowledge on the stochastic process of image formation and therefore can improve noise suppression. However, due to their iterative nature and the repeated forward- and back projection, such algorithms are computationally highly expensive, which poses a major limitation in particlar for interventional applications. The recent invention of machine-learning- and data-driven-based reconstruction methods can potentially provide opportunities for superior image quality and reconstruction speed comparable to MBIR techniques (Würfl *et al* 2016, Maier *et al* 2019, Russ *et al* 2022).

Several clinical prerequisites are needed to be considered while designing trajectory optimization frameworks. For instance, in the most of studies done in this field, an anatomical model which was an exact representation of the patient/object and did not consider potential uncertainty in realistic clinical scenarios e.g. regions of high attenuation within the patient due to contrast agent , surgical tools and unplanned embolization sites where were not accounted in the anatomical model of the patient. This introduces a limitation that can be explored further, for instance, by means of using probability distributions for the anatomical model and parameters which are defined for the imaging tasks (Capostagno *et al* 2019). Consequently, a distribution of trajectories from which a robust approximation of the group optimum could be selected. There are also several challenges when acquiring such non-circular data. For instance, a major barrier for the clinical translation of current and future extended FOV CBCT imaging techniques, especially in the interventional room, is limited vendor support. To date, novel trajectories implemented on clinical imaging hardware have required additional software or hardware control of the system provided by the vendor. One example of non-circular trajectories which has already been implemented in clinic is the Sine Spin orbit which has been implemented on Icono biplane C-arm system (Siemens Healthineers, Forchheim). The additional control often comes at the expense of system capabilities (i.e. limiting the gantry rotation and table translation speeds), limiting the ability to optimize the trajectories experimentally. In addition, manufacturers of the imaging technologies currently do not fully support the realization of arbitrary trajectories on their machines. As a consequence, the implementation of arbitrary trajectories on clinical CBCT machines is still an ongoing effort and still encounters major challenges e.g. robust calibration due to geometrical uncertainties of the CBCT machines. In addition, the velocity and acceleration constraints of C-arm machines need to be integrated into the design prior to translation of such non-conventional trajectories onto physical imaging systems.

One other important practical consideration for such trajectory optimization frameworks is that the methodology mainly assumes having a registered prior image for the trajectory design. Hence, a registration step is needed to have a practical workflow. This can be done using some initial projections and 2D/3D registration (Ouadah *et al* 2016). In this case, an adaptive on-the-fly trajectory design would be of potential benefit as then the trajectory can be adjusted to maximize the imaging performance.

Another future perspective can also be the expansion of optimization parameters in order to further improve the trajectory and overall imaging performance for instance a parallel optimization of the reconstruction parameters (regularization constants) as well as imaging factors (kV and mAs). Such a task-driven CBCT scanning procedure introduces a new paradigm for further improvement of image quality and/or reduction in the patient dose.

5. Conclusion

Customized CBCT trajectories offer the potential to improve imaging performance in the interventional room, they are a new approach for dose reduction and can enable imaging against complications in the operating theater. In industrial CT, customized CBCT trajectories enable scans of large-scale objects and allow image quality improvements. The current study focuses on the review and discussion of the available literature and developments in the area of CBCT trajectory optimization. This is the first study that provides a comprehensive literature review regarding proposed task-aware CBCT optimization algorithms and tries to update the research community with the thorough information on the recent progress and the future trends.

Acknowledgments

ORCID iDs

S Hatamikia ⓘ https://orcid.org/0000-0002-0182-0954
A Biguri ⓘ https://orcid.org/0000-0002-2636-3032
T Reynolds ⓘ https://orcid.org/0000-0003-0543-9170
T Russ ⓘ https://orcid.org/0000-0002-7476-3508
A Maier ⓘ https://orcid.org/0000-0002-9550-5284

References

Abul-Kasim K, Söderberg M, Selariu E, Gunnarsson M, Kherad M and Ohlin A 2012 Optimization of radiation exposure and image quality of the cone-beam o-arm intraoperative imaging system in spinal surgery *J. Spinal Disorders Tech.* **25** 52–8

Ametova E, Ferrucci M and Dewulf W 2017 A tool for reducing cone-beam artifacts in computed tomography data *7th Conf. on Industrial Computed Tomography*

Amirkhanov A, Heinzl C, Reiter M and Gröller E 2010 Visual optimality and stability analysis of 3DCT scan positions *IEEE Trans. Visual Comput. Graphics* **16** 1477–86

Barrett H H, Yao J, Rolland J P and Myers K J 1993 Model observers for assessment of image quality *Proc. Natl. Acad. Sci.* **90** 9758–65

Bauer F, Goldammer M and Grosse C U 2020 Scan time reduction by fewer projections-an approach for part-specific acquisition trajectories *20th World Conf. on Non-Destructive Testing*

Becker A E, Hernandez A M, Boone J M and Schwoebel P 2020 A prototype multi-x-ray-source array (MXA) for digital breast tomosynthesis *Phys. Med. Biol.* **65** 235033

Berris T, Gupta R and Rehani M M 2013 Radiation dose from cone-beam CT in neuroradiology applications *AJR Am. J. Roentgenol.* **200** 755–61

Boas F E and Fleischmann D 2012 CT artifacts: causes and reduction techniques *Imaging Med.* **4** 229–40

Boone J M, Becker A E, Hernandez A M, Dobbins J T and Schwoebel P 2019 Multi-x-ray source array for stationary tomosynthesis or multi-cone angle cone beam CT *Proc SPIE* **10948** 109480U

Brahme A, Nyman P and Skatt B 2008 4d laser camera for accurate patient positioning, collision avoidance, image fusion and adaptive approaches during diagnostic and therapeutic procedures *Med. Phys.* **35** 1670–81

Brierley N, Bellon C and Lazaro Toralles B 2018 Optimized multi-shot imaging inspection design *Proc. R. Soc.* A **474** 20170319

Buratti A, Ferrucci M, Achour S B, Dewulf W and Schmitt R H 2016 An analytical method for optimizing imaging parameters in industrial x-ray computed tomography for dimensional measurements on multimaterial workpieces *Proc SPIE* **9967** 99671C

Busser W M H, Braak S J, Fütterer J J, van Strijen M J L, Hoogeveen Y L, de Lange F and Schultze Kool L J 2013 Cone beam CT guidance provides superior accuracy for complex needle paths compared with CT guidance *Br. J. Radiol.* **86** 20130310

Butzhammer L, Müller A M and Hausotte T 2020 Comparison of geometrically derived quality criteria regarding optimal workpiece orientation for computed tomography measurements *10th Conf. on Industrial Computed Tomography*

Buzug T M 2010 *Computed Tomography: From Photon Statistics to Modern Cone-Beam CT* (Berlin: Springer) (https://doi.org/10.1007/978-3-540-39408-2)

Capostagno S, Stayman J W, Jacobson M, Ehtiati T, Weiss C R and Siewerdsen J H 2019 Task-driven source-detector trajectories in cone-beam computed tomography: Ii. application to neuroradiology *J. Med. Imaging (Bellingham, Wash.)* **6** 025004

Carrino J A *et al* 2014 Dedicated cone-beam ct system for extremity imaging *Radiology* **270** 816–24

Choi J-H, Fahrig R, Keil A, Besier T F, Pal S, McWalter E J, Beaupré G S and Maier A 2013 Fiducial marker-based correction for involuntary motion in weight-bearing C-arm CT scanning of knees. part I. numerical model-based optimization *Med. Phys.* **40** 091905

Choi J-H, Maier A, Keil A, Pal S, McWalter E J, Beaupré G S, Gold G E and Fahrig R 2014 Fiducial marker-based correction for involuntary motion in weight-bearing C-arm CT scanning of knees. ii. experiment *Med. Phys.* **41** 061902

Chung K, Schad L R and Zöllner F G 2018 Tomosynthesis implementation with adaptive online calibration on clinical c-arm systems *Int. J. Comput. Assist. Radiol. Surg.* **13** 1481–95

Claus B E H, Langan D A, Al Assad O and Wang X 2015 Circular tomosynthesis for neuro perfusion imaging on an interventional c-arm *Proc SPIE* **9412** 94122A

Cormack A M 1963 Representation of a function by its line integrals, with some radiological applications *J. Appl. Phys.* **34** 2722–7

Davis A M, Pearson E A, Pan X, Pelizzari C A and Al-Hallaq H A 2019 Collision-avoiding imaging trajectories for linac mounted cone-beam CT *J. X-Ray Sci. Technol.* **27** 1–16

Demehri S *et al* 2014 Assessment of image quality in soft tissue and bone visualization tasks for a dedicated extremity cone-beam ct system *Eur. Radiol.* **25** 1742–51

Feldkamp L A, Davis L C and Kress J W 1984 Practical cone-beam algorithm *J. Opt. Soc. Am.* A **1** 612–9

Fessler J A 1996 Mean and variance of implicitly defined biased estimators (such as penalized maximum likelihood): applications to tomography *IEEE Trans. Image Process.* **5** 493–506

Fessler J A 2006 Image reconstruction: algorithms and analysis (https://doi.org/10.1.1.459.2975)

Fessler J A and Rogers W L 1996 Spatial resolution properties of penalized-likelihood image reconstruction: space-invariant tomographs *IEEE Trans. Image Process.* **5** 1346–58

Fischer A, Lasser T, Schrapp M, Stephan J and Noël P B 2016 Object specific trajectory optimization for industrial x-ray computed tomography *Sci. Rep.* **6** 19135

Gang G J, Lee J, Stayman J W, Tward D J, Zbijewski W, Prince J L and Siewerdsen J H 2011 Analysis of fourier-domain task-based detectability index in tomosynthesis and cone-beam CT in relation to human observer performance *Med. Phys.* **38** 1754–68

Gang G J, Russ T, Ma Y, Toennes C, Siewerdsen J H, Schad L R and Stayman J W 2020 Metal-tolerant noncircular orbit design and implementation on robotic C-arm systems *Int. Conf. on Image Formation in X-Ray Computed Tomography* vol 2020 pp 400–3 Conference proceedings

Gang G J, Siewerdsen J H and Stayman J W 2020 Non-circular CT orbit design for elimination of metal artifacts *Proc. of SPIE–the Int. Society for Optical Engineering*11312

Gang G J, Stayman J W, Ehtiati T and Siewerdsen J H 2015 Task-driven image acquisition and reconstruction in cone-beam CT *Phys. Med. Biol.* **60** 3129–50

Gang G J, Stayman J W, Ehtiati T and Siewerdsen J H 2015 Task-driven image acquisition and reconstruction in cone-beam ct *Phys. Med. Biol.* **60** 3129–50

Gang G J, Zbijewski W, Mahesh M, Thawait G, Packard N J, Yorkston J, Demehri S and Siewerdsen J H 2018 Image quality and dose for a multisource cone-beam CT extremity scanner *Med. Phys.* **45** 144–55

Gordon R and Herman G T 1974 Three-dimensional reconstruction from projections: a review of algorithms *Int. Rev. Cytol.* **38** 111–51

Grozmani N, Buratti A and Schmitt R H 2019 Investigating the influence of workpiece placement on the uncertainty of measurements in industrial computed tomography *9th Conf. on Industrial Computed Tomography*

Guo Z, Lauritsch G, Maier A K, Kugler P, Islam M K, Vogt F and Noo F 2020 C-arm CT imaging with the extended line-ellipse-line trajectory: first implementation on a state-of-the-art robotic angiography system *Phys. Med. Biol.* **65** 185016

Gupta R, Grasruck M, Suess C, Bartling S H, Schmidt B, Stierstorfer K, Popescu S, Brady T and Flohr T 2006 Ultra-high resolution flat-panel volume CT: fundamental principles, design architecture, and system characterization *Eur. Radiol.* **16** 1191–205

Hansen N and Kern S 2004 Evaluating the cma evolution strategy on multimodal test functions *Int. Conf. on Parallel Problem Solving from Nature*

Hatamikia S 2021 Patient specific source-detector trajectory optimization for cone beam computed tomography *PhD Thesis* Medical University of Vienna

Hatamikia S, Biguri A, Kronreif G, Figl M, Russ T, Kettenbach J, Buschmann M and Birkfellner W 2021 Toward on-the-fly trajectory optimization for C-arm CBCT under strong kinematic constraints *PLoS One* **16** e0245508

Hatamikia S, Biguri A, Kronreif G, Furtado H, Buschmann M, Kettenbach J, Steiner E, Gober M, Georg D and Birkfellner W 2020 Po-1701: optimized source-detector trajectories for low dose CBCT *Radiother. Oncol.* **152** S937–S938

Hatamikia S, Biguri A, Kronreif G, Kettenbach J, Russ T and Birkfellner W 2022 Possibility assessment of CBCT metal artifact reduction based on PICCS reconstruction and trajectory optimization *Proc SPIE* **12034** 120340W

Hatamikia S, Biguri A, Kronreif G, Russ T, Kettenbach J and Birkfellner W 2020 Short scan source-detector trajectories for target-based CBCT *2020 42nd Annual Int. Conf. of the IEEE Engineering in Medicine & Biology Society (EMBC)* pp 1299–302

Hatamikia S *et al* 2020 Optimization for customized trajectories in cone beam computed tomography *Med. Phys.* **47** 4786–99

Herbst M, Schebesch F, Berger M, Choi J-H, Fahrig R, Hornegger J and Maier A 2015 Dynamic detector offsets for field of view extension in c-arm computed tomography with application to weight-bearing imaging *Med. Phys.* **42** 2718–29

Herl G, Hiller J and Maier A 2020 Scanning trajectory optimisation using a quantitative tuybased local quality estimation for robot-based X-ray computed tomography *Nondestruct. Test. Eval.* **35** 287–303

Herl G, Hiller J and Sauer T 2019 Artifact reduction in x-ray computed tomography by multipositional data fusion using local image quality measures *9th Conf. on Industrial Computed Tomography*

Herl G, Hiller J, Thies M, Zaech J-N, Unberath M and Maier A 2021 Task-specific trajectory optimisation for twin-robotic x-ray tomography *IEEE Trans. Comput. Imaging* **7** 894–907

Herl G, Rettenberger S, Hiller J and Sauer T 2018 Metal artifact reduction by fusion of CT scans from different positions using the unfiltered backprojection *8th Conf. on Industrial Computed Tomography*

Hounsfield G N 1973 Computerized transverse axial scanning (tomography). 1. description of system *Br. J. Radiol.* **46** 1016–22

Hua C, Yao W, Kidani T, Tomida K, Ozawa S, Nishimura T, Fujisawa T, Shinagawa R and Merchant T E 2017 A robotic C-arm cone beam CT system for image-guided proton therapy: design and performance *Br. J. Radiol.* **90** 20170266

Humm J L, Pizzuto D, Fleischman E and Mohan R 1995 Collision detection and avoidance during treatment planning *Int. J. Radiat. Oncol., Biol., Phys.* **33** 1101–8

Jacobson M W *et al* 2018 A line fiducial method for geometric calibration of cone-beam CT systems with diverse scan trajectories *Phys. Med. Biol.* **63** 025030

Jaffray D A and Siewerdsen J H 2000 Cone-beam computed tomography with a flat-panel imager: initial performance characterization *Med. Phys.* **27** 1311–23

Jaffray D A, Siewerdsen J H, Wong J W and Martinez A A 2002 Flat-panel cone-beam computed tomography for image-guided radiation therapy *Int. J. Radiat. Oncol., Biol., Phys.* **53** 1337–49

Jaszczak R J 2006 The early years of single photon emission computed tomography (SPECT): an anthology of selected reminiscences *Phys. Med. Biol.* **51** R99–115

Je U, Cho H, Lee M, Oh J-E, Park Y, Hong D-K, Park C, Cho H, Choi S and Koo Y 2014 Dental cone-beam CT reconstruction from limited-angle view data based on compressed-sensing (CS) theory for fast, low-dose x-ray imaging *J. Korean Phys. Soc.* **64** 1907–11

Jones K O 2006 Comparison of genetic algorithms and particle swarm optimization for fermentation feed profile determination *Int. Conf. On Computer Systems and Technologies*

Kak A C and Slaney M 2001 *Classics in Applied Mathematics: Principles of Computerized Tomographic Imaging* (Philadelphia, PA: SIAM) (https://doi.org/10.1137/1.9780898719277)

Kalender W A, Seissler W, Klotz E and Vock P 1990 Spiral volumetric CT with single-breath-hold technique, continuous transport, and continuous scanner rotation *Radiology* **176** 181–3

Kauffmann C, Douane F, Thérasse É, Lessard S, Elkouri S, Gilbert P J, Beaudoin N, Pfister M, Blair J F and Soulez G 2015 Source of errors and accuracy of a two-dimensional/three-dimensional fusion road map for endovascular aneurysm repair of abdominal aortic aneurysm *J. Vas. Interventional Radiol.: JVIR* **26** 544–51

Kleinjan G H, van den Berg N S, van Oosterom M N, Wendler T, Miwa M, Bex A, Hendricksen K, Horenblas S and van Leeuwen F W B 2016 Toward (hybrid) navigation of a fluorescence camera in an open surgery setting *J. Nuclear Med.* **57** 1650–53

Kohler Th, Proksa R and Grass M 2001 A fast and efficient method for sequential cone-beam tomography *Med. Phys.* **28** 2318–27

Kuhl D and Edwards R Q 1970 The mark III scanner: a compact device for multiple-view and section scanning of the brain *Radiology* **96** 563–70

Ladikos A, Benhimane S and Navab N 2008 Real-time 3D reconstruction for collision avoidance in interventional environments. Medical image computing and computer-assisted intervention *MICCAI Int. Conf. on Medical Image Computing and Computer-Assisted Intervention* vol 11, pp 526–34

Li T, Li X, Yang Y, Heron D E and Saiful Huq M 2010 A novel off-axis scanning method for an enlarged ellipse cone-beam computed tomography field of view *Med. Phys.* **37** 6233–9

Lu B, Lu H and Palta J R 2010 A comprehensive study on decreasing the kilovoltage cone-beam CT dose by reducing the projection number *J. Appl. Clin. Med. Phys.* **11** 231–49

Lu Y, Yang J, Emerson J W, Mao H, Zhou T, Si Y and Jiang M 2012 Cone-beam reconstruction for the two-circles-plus-one-line trajectory *Phys. Med. Biol.* **57** 2689–707

Maier A, Choi J-H, Keil A, Niebler C, Sarmiento M, Fieselmann A, Gold G, Delp S and Fahrig R 2011 Analysis of vertical and horizontal circular C-arm trajectories *Med. Imaging 2011: Phys. Med. Imaging* **7961** 602–9 SPIE

Maier A, Kugler P, Lauritsch G and Hornegger J 2015 Discrete estimation of data completeness for 3D scan trajectories with detector offset *Bildverarbeitung für die Med.* **2015** 47–52 Springer

Maier A, Steidl S, Christlein V and Hornegger J 2018 *Medical Imaging Systems: an Introductory Guide* (Berlin: Springer)

Maier A, Syben C, Lasser T and Riess C 2019 A gentle introduction to deep learning in medical image processing *Z. für Med. Phys.* **29** 86–101

Manhart M, Dennerlein F and Kunze H 2010 Online cone beam reconstruction with displaced flat panel detector *Proceedings of the First International Conference on Image Formation in X-Ray Computed* ed F Noo (UT: Salt Lake City) pp 53–5 2010

Mann T D, Ploquin N, Gill W A and Thind K 2019 Development and clinical implementation of eclipse scripting-based automated patient-specific collision avoidance software *J. Appl. Clin. Med. Phys.* **20** 12–9

Meng B, Xing L, Han B, Koong A C, Chang D T, Cheng J C-H and Li R 2013 Cone beam CT imaging with limited angle of projections and prior knowledge for volumetric verification of non-coplanar beam radiation therapy: a proof of concept study *Phys. Med. Biol.* **58** 7777–89

Mohamathu Rafic K, Balasingh Timothy Peace S, Manu M, Arvind S and Paul Ravindran B 2019 A rationale for cone beam CT with extended longitudinal field-of-view in image guided adaptive radiotherapy *Phys. Med.: PM : Int. J. Devoted Appl. Phys. Med. Biol.: Official J. Ital. Assoc. Biomed. Phys.* **62** 129–39

Muehllehner G 1971 A tomographic scintillation camera *Phys. Med. Biol.* **16** 87–96

Muehllehner G and Wetzel R 1971 Section imaging by computer calculation *J. Nucl. Med.* **12** 76–84

Nett B, Zambelli J, Riddell C, Belanger B F and Madison Chen G-H 2007 Circular tomosynthesis implemented with a clinical interventional flat-panel based c-arm: initial performance study *SPIE Med. Imaging* **6510** 6510N

Noo F and Kachelriess M 2019 Advances and trends in image formation in x-ray CT *Med. Phys.* **44** e112

Ouadah S, Stayman J W, Gang G J, Ehtiati T and Siewerdsen J H 2016 Self-calibration of cone-beam CT geometry using 3D-2D image registration *Phys. Med. Biol.* **61** 2613–32

Pack J D, Noo F and Clackdoyle R 2005 Cone-beam reconstruction using the backprojection of locally filtered projections *IEEE Trans. Med. Imaging* **24** 70–85

Padilla L, Pearson E A and Pelizzari C A 2015 Collision prediction software for radiotherapy treatments *Med. Phys.* **42** 6448–56

Pearson E A, Cho S, Pelizzari C A and Pan X 2010 Non-circular cone beam CT trajectories: a preliminary investigation on a clinical scanner *IEEE Nuclear Science Symp & Medical Imaging Conf.* pp 3172–5

Pelc N J and Chesler D A 1979 Utilization of cross-plane rays for three-dimensional reconstruction by filtered back-projection *J. Comput. Assist. Tomogr.* **3** 385–95

Peters T M, Smith P R and Gibson R D 1973 Computer aided transverse body-section radiography *Br. J. Radiol.* **46** 314–7

Powell M F, Dinobile D and Reddy A S 2010 C-arm fluoroscopic cone beam CT for guidance of minimally invasive spine interventions *Pain Physician* **13** 51–9

Pung L, Ahmad M, Mueller K, Rosenberg J, Stave C D, Hwang G L, Shah R P and Kothary N 2017 The role of cone-beam CT in transcatheter arterial chemoembolization for hepatocellular carcinoma: a systematic review and meta-analysis *J. Vasc. Interventional Radiol.: JVIR* **28** 334–41

Radon J 1917 Über die Bestimmung von Funktionen durch ihre Integralwerte längs gewisser Mannigfaltigkeiten *Ber. über die Verh. der Sächsische Akad. der Wiss.* **69** 262–77 00000

Reisinger S, Kasperl S, Franz M, Hiller J and Schmid U 2011 Simulation-based planning of optimal conditions for industrial computed tomography *Int. Symp. on Digital Industrial Radiology and Computed Tomography*

Reynold T *et al* 2021 Understanding collateral evolution in Linux device drivers *Proc. of the in Annual Meeting of the American Association of Physicists*

Reynolds T *et al* 2022 Extended intraoperative longitudinal 3-dimensional cone beam computed tomography imaging with a continuous multi-turn reverse helical scan *Investigative Radiol.* (https://doi.org/10.1097/RLI.0000000000000885)

Richter P H, Yarboro S R, Kraus M and Gebhard F 2015 One year orthopaedic trauma experience using an advanced interdisciplinary hybrid operating room *Injury* **46** S129–34

Roxby P, Kron T, Foroudi F, Haworth A, Fox C, Mullen A and Cramb J A 2009 Simple methods to reduce patient dose in a varian cone beam CT system for delivery verification in pelvic radiotherapy *Br. J. Radiol.* **82** 855–9

Russ T *et al* 2022 Fast CBCT reconstruction using convolutional neural networks for arbitrary robotic C-arm orbits *Med. Imaging 2022: Image-Guided Proced., Robot. Interventions, Model.* **12031** 120311I

Schielein R, Scholz G, Wagner R, Kretzer C, Fuchs T, Kasperl S, Bär F, Kirsch S, Zepf M and Wolters-Rosbach M 2016 The musices project: simulative automated CT acquisition planning for historical brass instruments improves image quality *6th Conf. on Industrial Computed Tomography*

Schmitt R, Isenberg C and Niggemann C 2012 Knowledge-based system to improve dimensional CT measurements *4th Conf. on Industrial Computed Tomography*

Seifert H, Hagen T, Bartylla K, Blass G and Piepgras U 1997 Patient doses from standard and spiral CT of the head using a fast twin-beam system *Br. J. Radiol.* **70** 1139–45

Setser R, Chintalapani G, Bhadra K and Casal R F 2020 Cone beam CT imaging for bronchoscopy: a technical review *J. Thoracic Dis.* **12** 7416–28

Shannon C E 1949 Communication in the presence of noise *Proc. IRE* **37** 10–21

Sidky E Y, Pan X, Reiser I S, Nishikawa R M, Moore R H and Kopans D B 2009 Enhanced imaging of microcalcifications in digital breast tomosynthesis through improved image-reconstruction algorithms *Med. Phys.* **36** 4920–32

Siewerdsen J H, Uneri A, Muñoz Hernández A, Burkett G and Boone J M 2019 Cone-beam ct dose and imaging performance evaluation: with a modular, multi-purpose phantom *Med. Phys.* **47** 467–79

Sohn J J, Kim C, Kim D H, Lee S-R, Zhou J, Yang X and Liu T 2020 Analytical low-dose CBCT reconstruction using non-local total variation regularization for image guided radiation therapy *Front. Oncol.* **10** 242

Stayman J W, Capostagno S, Gang G J and Siewerdsen J H 2019 Task-driven source-detector trajectories in cone-beam computed tomography: I. theory and methods *J. Med. Imaging (Bellingham, Wash.)* **6** 025002

Stayman J W, Gang G J and Siewerdsen J H 2015 Task-based optimization of source-detector orbits in interventional cone-beam CT *Proc. Int. Meet. Fully Three-Dimensional Image Reconstruct. in Radiol. and Nucl. Med*

Stayman J W and Siewerdsen J H 2013 Task-based trajectories in iteratively reconstructed interventional cone-beam CT *Proc. 12th Int. Meet. Fully Three-Dimensional Image Reconstr. Radiol. Nucl. Med* pp 257–60

Stevens G M, Birdwell R L, Beaulieu C F, Ikeda D M and Pelc N J 2003 Circular tomosynthesis: potential in imaging of breast and upper cervical spine-preliminary phantom and in vitro study *Radiology* **228** 569–75

Stock M, Palm A, Altendorfer E, Steiner and Georg D 2012 Igrt induced dose burden for a variety of imaging protocols at two different anatomical sites *Radiother. Oncol.: J. Eur. Soc. Ther. Radiol. Oncol.* **102** 355–63

Stromer D, Amrehn M, Huang Y, Kugler P, Bauer S, Lauritsch G and Maier A 2016 Comparison of sart and etv reconstruction for increased C-arm CT volume coverage by proper detector rotation in liver imaging *2016 IEEE 13th Int. Symp. on Biomedical Imaging (ISBI), IEEE* pp 589–92

Stromer D, Kugler P, Bauer S, Lauritsch G and Maier A 2016 Data completeness estimation for 3D c-arm scans with rotated detector to enlarge the lateral field-of-view *Bildverarbeitung für die Medizin 2016* (Berlin: Springer) pp 164–9

Sun W Z, Wang B, Qiu B, Liang J, Xie W, Deng X and Qi Z Y 2017 Assessment of female breast dose for thoracic cone-beam CT using mosfet dosimeters *Oncotarget* **8** 20179–86

Tam K 1997 Cone beam imaging of a section of a long object with a short detector *International Conference on Information Processing in Medical Imaging, IPMI 1997* pp 525–30

Tan J, Li H, Klein E E, Li H, Parikh P J and Yang D 2012 Physical phantom studies of helical cone-beam CT with exact reconstruction *Med. Phys.* **39** 4695–704

Tersol A, Wu P, Clackdoyle R, Boone J M and Siewerdsen J H 2022 Sampling effects for emerging cone-beam CT systems and scan trajectories: from tuy's condition to system design and routine image quality tests *Medical Imaging: Physics of Medical Imaging* (SPIE)

Thies M, Zäch J-N, Gao C, Taylor R H, Navab N, Maier A K and Unberath M 2020 A learning-based method for online adjustment of C-arm cone-beam CT source trajectories for artifact avoidance *Int. J. Comput. Assist. Radiol. Surg.* **15** 1787–96

Tuy H K 1983 An inversion formula for cone-beam reconstruction *SIAM J. Appl. Math.* **43** 546–52

Verdun F R, Racine D, Ott J G, Tapiovaara M J, Toroi P, Bochud F O, Veldkamp W J H, Schegerer A, Bouwman R W and Hernandez Giron I 2015 Image quality in CT: from physical measurements to model observers *Phys. Med.* **31** 823–43

Wang A S, Webster Stayman J, Otake Y, Kleinszig G, Vogt S, Gallia G L, Khanna A J and Siewerdsen J H 2014 Soft-tissue imaging with c-arm cone-beam CT using statistical reconstruction *Phys. Med. Biol.* **59** 1005–26

Wang J, Li T, Liang Z and Xing L 2008 Dose reduction for kilovotage cone-beam computed tomography in radiation therapy *Phys. Med. Biol.* **53** 2897–909

Webb S 1990 *From the Watching of Shadows: The Origins of Radiological Tomography* (Boca Raton, FL: CRC Press)

Wu P *et al* 2020 C-arm non-circular orbits: geometric calibration, image quality, and avoidance of metal artifacts arXiv:2010.00175

Wu P *et al* 2020 C-arm orbits for metal artifact avoidance (MAA) in cone-beam CT *Phys. Med. Biol.* **65** 165012

Würfl T, Ghesu F C, Christlein V and Maier A 2016 Deep learning computed tomography *Int. Conf. on Medical Image Computing and Computer-Assisted Intervention, Springer* pp 432–40

Xue L and Suzuki H 2017 Evaluation of scanning parameters based on image entropy for dimensional computed tomography metrology *J. Manuf. Sci. Eng.* **139** 071001

Yang D, Li H H, Goddu S M and Tan J 2014 CBCT volumetric coverage extension using a pair of complementary circular scans with complementary kv detector lateral and longitudinal offsets *Phys. Med. Biol.* **59** 6327–39

Yoo J, Schafer S, Uneri A, Otake Y, Khanna A J and Siewerdsen J H 2013 An electromagnetic 'tracker-in-table' configuration for x-ray fluoroscopy and cone-beam CT-guided surgery *Int. J. Comput. Assist. Radiol. Surg.* **8** 1–13

Yu V Y, Tran A, Nguyen D, Cao M, Ruan D, Low D A and Sheng K 2015 The development and verification of a highly accurate collision prediction model for automated noncoplanar plan delivery *Med. Phys.* **42** 6457–67

Yu Z, Lauritsch G, Dennerlein F, Mao Y, Hornegger J and Noo F 2016 Extended ellipse-line-ellipse trajectory for long-object cone-beam imaging with a mounted c-arm system *Phys. Med. Biol.* **61** 1829–51

Yu Z, Lauritsch G, Hornegger J and Noo F 2014 Efficient and exact C-arm cone-beam imaging for axially extended field-of-view using the ellipse-line-ellipse trajectory *Proc. of The Third Int. Conf. on Image Formation in X-Ray Computed Tomography (Salt Lake City, USA)* pp 311–4

Yu Z, Maier A, Lauritsch G, Vogt F, Schönborn M, Köhler C, Hornegger J and Noo F 2014 Axially extended-volume C-arm CT using a reverse helical trajectory in the interventional room *IEEE Trans. Med. Imaging* **34** 203–15

Yu Z, Maier A, Lauritsch G, Vogt F, Schönborn M, Köhler C, Hornegger J and Noo F 2014 Image quality assessment for extended-volume C-arm CT using a multi-turn reverse helix *2014 IEEE Nuclear Science Symp. and Medical Imaging Conf. (NSS/MIC)* pp 1–4 IEEE

Yu Z, Maier A K, Lauritsch G, Vogt F, Schonborn M, Kohler C, Hornegger J and Noo F 2015 Axially extended-volume C-arm CT using a reverse helical trajectory in the interventional room *IEEE Trans. Med. Imaging* **34** 203–15

Yu Z, Noo F, Dennerlein F, Lauritsch G and Hornegger J 2010 X-ray source trajectories and their r-line coverage for long-object CB imaging with a C-arm system *Proc. of The First Int. Conf on Image Formation in X-ray Computed Tomography* pp 175–80

Yu Z, Noo F, Dennerlein F, Lauritsch G and Hornegger J 2011 FDK-type reconstruction algorithms for the reverse helical trajectory *2011 IEEE Nuclear Science Symp. Conf. Record* pp 3980–5 IEEE

Yu Z, Noo F, Lauritsch G and Hornegger J 2013 Extended-volume image reconstruction using the ellipse-line-ellipse trajectory for a C-arm system *Proc. of the 12th Int. Meeting on Fully Three-Dimensional Image Reconstruction in Radiology and Nuclear Medicine* pp 245–8

Yu Z, Wunderlich A, Dennerlein F, Lauritsch G and Noo F 2011 Line plus arc source trajectories and their R-line coverage for long-object cone-beam imaging with a C-arm system *Phys. Med. Biol.* **56** 3447–71

Zabler S, Maisl M, Hornberger P, Hiller J, Fella C and Hanke R 2021 X-ray imaging and computed tomography for engineering applications *tm-Technisches Messen* **88** 211–26

Zaech J-N, Gao C, Bier B, Taylor R, Maier A, Navab N and Unberath M 2019 Learning to avoid poor images: Towards task-aware C-arm cone-beam CT trajectories *Int. Conf. on Medical Image Computing and Computer-Assisted Intervention* (Berlin: Springer) pp 11–9

Zbijewski W *et al* 2011 A dedicated cone-beam ct system for musculoskeletal extremities imaging: design, optimization, and initial performance characterization *Med. Phys.* **38** 4700–13

Zeng G L and Gullberg G T 1992 A cone-beam tomography algorithm for orthogonal circle-and-line orbit *Phys. Med. Biol.* **37** 563–77

Zhao C, Herbst M, Vogt S, Ritschl L, Kappler S, Siewerdsen J H and Zbijewski W 2019 A robotic x-ray cone-beam CT system: trajectory optimization for 3D imaging of the weight-bearing spine *Proc SPIE* **10948** 109481L

Zheng D, Lu J, Jefferson A, Zhang C, Wu J, Sleeman W C, Weiss E, Dogan N, Song S and Williamson J F 2012 A protocol to extend the longitudinal coverage of on-board cone-beam CT *J. Appl. Clin. Med. Phys.* **13** 141–51

Zou W, Lin H, Plastaras J P, Wang H C, Bui V, Vapiwala N, Mcdonough J E, Tochner Z A and Both S 2012 A clinically feasible method for the detection of potential collision in proton therapy *Med. Phys.* **39** 7094–101